Scuola Internazionale di Studi Superiori Avanzati

International School for Advanced Studies

- T R I E S T E -

Giovanni Vladilo

PHYSICAL PROCESSES IN THE LOCAL INTERSTELLAR MEDIUM

Tesi di Magister Philosophiae

Relatore: Prof. John E. Beckman

Anno Accademico 1985/1986

INDEX

INTRODUCTION

The Interstellar Medium (ISM) is a very interesting laboratory of physics and physico-chemistry showing a vast range of physical parameters. A wide variety of interesting phenomena can be studied in the ISM, often in conditions far from thermodynamic equilibrium: ionization and recombination, excitation of atomic and molecular levels, spectral line formation, thermal exchanges, hydrodynamic phenomena (including shocks), condensation and destruction of grains, formation and destruction of molecules, etc.

The ISM plays a major role in the evolution of galaxies. Galaxies contains up to 40% of their mass as interstellar gas and dust. Stars are born from this interstellar medium and return continuosly to it matter enriched in heavy elements by nucleo-synthesis. Moreover exchanges of interstellar gas between different parts of a galaxy and exchanges with the intergalactic medium are likely to modify strongly this simple picture of galactic evolution.

When we try to derive the global properties of the ISM on a large scale - i.e., making observations along lines of sight ranging from some hundreds parsecs to some kiloparsecs - we must face the problem that we are averaging structures with different sizes and physical properties, and that we are not sure of which physical processes are relevant in each region. The fact that long lines of sight generally intersect many components of each of the several phases of the interstellar gas, makes especially complicated the interpretation of the observed spectral features. Moreover, the lines of sight can intersect circumstellar regions with physical conditions different

from those existing in the diffuse ISM, such as Stromgren spheres of hot stars (characterized by strong UV radiation fields) or interfaces between stellar winds and ISM (characterized by particular collisional processes).

For these reasons, the study of the ISM along short lines of sight - i.e., within a volume of radius less than 100-200 pc - offers advantages which make the Local Interstellar Medium (LISM) a convenient framework for studies of the physics of the general interstellar space. The LISM is a laboratory where we can to try to decide on the relative importance of various physical processes, taking advantage from detailed observations of nearby regions. The exploration of short lines of sight increases the probability of sampling regions with homogeneous physical properties.

If we study interstellar absorption lines towards stars situated within a few tens of parsecs - as it is the case of the work discussed in this Thesis - we have the advantage of an accurate determination of the distances to the targets and, as a consequence, of the mean density of the gas along the line of sight, which is an important indicator of its physical state.

Apart from these advantages, the study of the LISM is important because the distribution of neutral hydrogen in the solar neighbourhood governs the transparency of the interstellar gas in the extreme ultraviolet, which is critical for the success of any future experiment in this spectral band (see Fig. 1).

Finally, the knowledge of the physical state of the LISM is important to understand the physical processes which occur at the

FIGURE 1

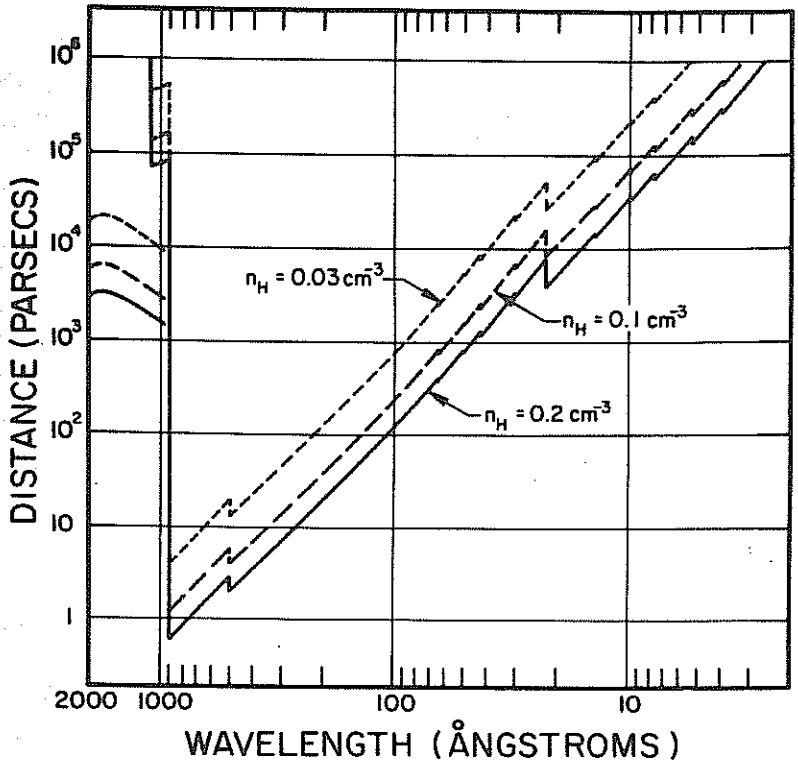

Distance at which 90% of the radiation emitted by an EUV source is absorbed in a neutral LISM phase as a function of wavelength (from Paresce, IAU Coll. 81, NASA CP 2345, 169).

interface between the solar wind and the nearby interstellar gas. A clear understaning of these interactions is the key to interpret correctly the observations of the interplanetary gas in order to deduce the physical properties of the gas in the solar neighbourhood.

The LISM is relatively difficult to explore due to the limited effects that it produces on the spectra of nearby stars. Only recently, thanks to UV and X-ray space-borne observations and progress in ground based observational techniques, it has become possible to draw a global picture of the local gas. In the First Part of this Thesis I review the observations of the LISM carried on in the different bands of the electromagnetic spectrum and by measurements in the interplanetary medium. In the Second Part current models for the general ISM and for the different phases of the LISM are briefly reviewed. Finally, in the Third Part, I report the results of an original study of the kinematics, distribution and physical state of the LISM within a few tens of parsecs. These results are discussed within the general context delined in the first two Parts.

FIRST PART

OBSERVATIONS OF THE LOCAL INTERSTELLAR MEDIUM

1. OPTICAL AND ULTRAVIOLET ABSORPTION LINES

Despite the numerous ways to study the ISM, the optical and the UV absorption lines are among the most powerful tools for observing the interstellar gas. Absorption lines give direct measurements of the column densities of a variety of elements in a number of ionization stages. In addition, they provide distance limits on the sampled material and give information on the velocity structure, density an inhomogeneity. However, target stars must be of suitable spectral type, preferably with high rotational velocities, to avoid confusion with stellar lines. The small number of targets generally limits the amount of spatial information that can be derived. In particular, the study of the LISM is complicated because of the very small number of early-type stars in a radius of about 100 pc from the sun.

Neutral gas observations

The low spatial density of early-type stars makes it necessary to use cool stars to probe the distribution of the interstellar gas within a few tens of parsecs. Cool stars are very numerous in the solar neighbourhood and their chromospheric emissions can provide a suitable background against which measure some interstellar absorptions. HI column densities towards nearby stars have been obtained by means of the Copernicus spectrometer, observing the interstellar absorption

superposed to the broad Lyα emission arising from the stellar chromosphere (McClintock et al. 1978, Anderson and Weiler 1978). Due to the limited sensitivity of the the Copernicus instrument, it was possible to perform direct HI measurements only towards a dozen cool stars closer than 20 pc. More recently, also the IUE satellite has been used to perform the same kind of measurements (see Murthy et al. 1986). Interstellar Lyα measurements in cool stars strongly depend on the selected chromospheric model and on the line-of-sight velocity dispersion of the gas (microturbulence parameter b). In order to derive information from the absorption line, a theoretical profile is fitted using as parameters the hydrogen density n(HI) and the parameter b (which is related to gas kinetic temperature). The fit on the observed profile also gives information on the bulk velocity of the gas. Murthy et al. (1986) find that the ISM along the lines of sight to several nearby stars is consistent with a local cloud of n(HI) $\sim$ 0.1 cm^{-3} and kinetic temperature T $\sim$ 10^4 K. The bulk velocities along the different lines of sight are consistent with an interstellar wind coming from the general direction of the galactic center, and are clearly not due to the motion of the sun in the Local Standard of Rest (LSR).

The uncertainties in the HI column densities derived by means of the Lyα observations can reach almost one order of magnitude and the observations can be performed only towards a limited sample of very nearby stars. For this reason it is very important to use different atomic species to sample the local interstellar gas. The small column densities typical of the short lines of sight within the LISM, make it necessary to use the resonance lines of the most abundant ions.

Taking into account the cosmic abundances of the elements, and the fact that, even in HI regions, the elements with ionization potential IP < 13.6 eV are mainly photoionized in the ISM, the ions most suitable for the detection of weak interstellar absorptions are: CII, NI, OI, MgII, SiII and FeII. Most of these ions produce chromospheric emissions in cool stars, but, with the exception of MgII, the lines fall in a UV spectral range where it is difficult to perform high resolution spectroscopy with late-type stars. In the Third Part of this Thesis I will discuss our own observations of interstellar MgII towards nearby cool stars.

Crutcher (1982) made an analysis of the radial velocities of the optical interstellar absorptions published by Stokes (1978). Using a simple kinematical model (uniform motion of the LISM with respect to the sun), and restricting his attention to the stars within 100 pc in Stokes's compilation, he made a best fit between the observed radial velocities and those predicted by the model, leaving as free parameters the direction and the magnitude of the LISM velocity. He found that the LISM is moving with respect to the sun at a velocity of -28 km/s from the galactic direction $l = 25^{\circ}$, $b = +10^{\circ}$. A fraction of this velocity is simply a reflection of the solar motion in the LSR. Taking into account this effect, it comes out that the LISM is moving at a velocity of -15 km/s from $l = 345^{\circ}$, $b = -10$ with respect to the LSR.

Frisch and York (1983) collect the results of satellite UV observations of neutral interstellar gas in front of 140 stars 10 - 3000 pc distant. In Fig. I.1.1 these results are shown projected onto representations of the galactic plane and of a plane passing through

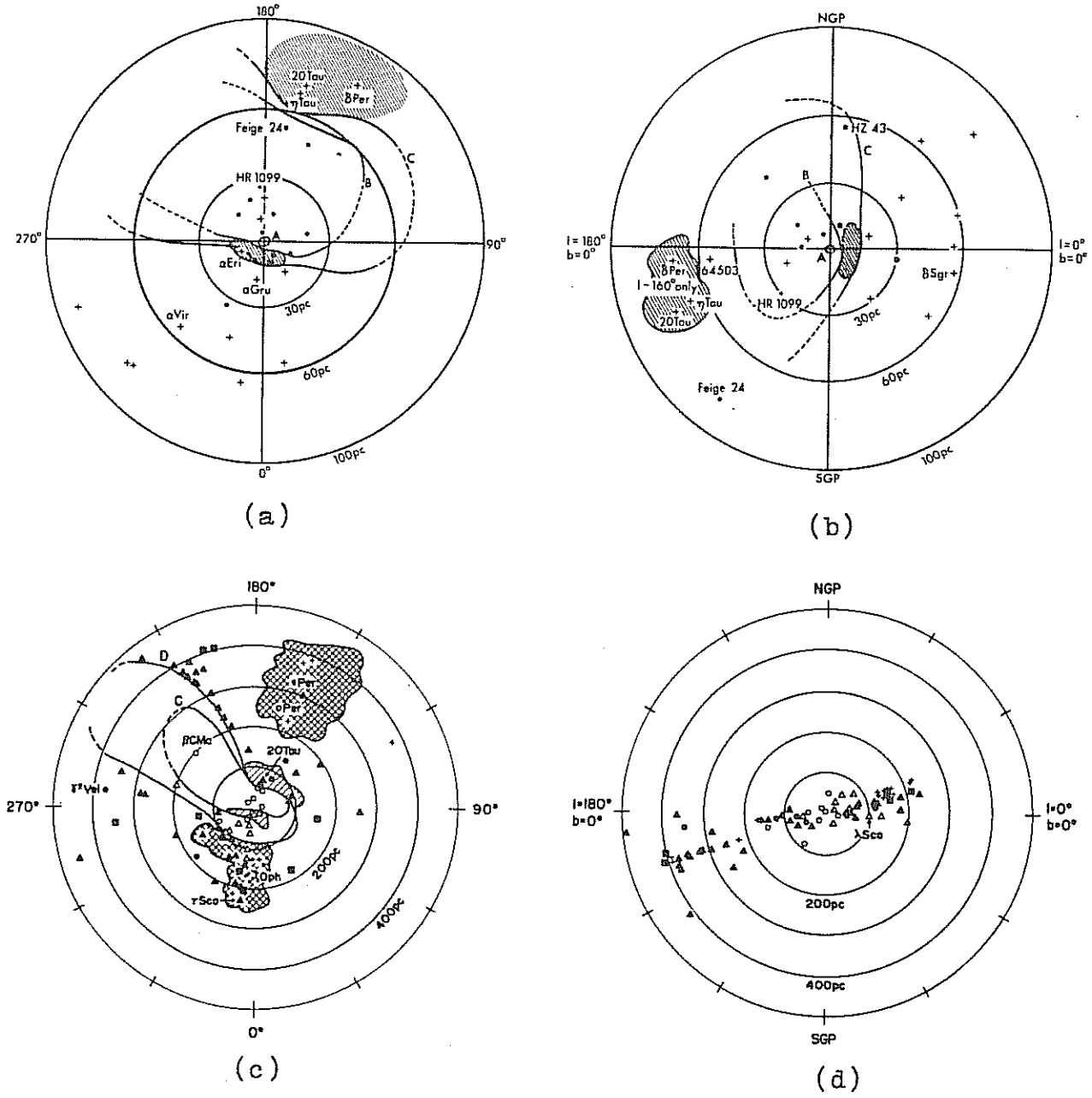

Fig. I.1.1 - Stars projected onto the galactic plane (a,c) and a plane passing through the poles and center-anticenter (b,d). Contour A: $N(H)\sim 5\times10^{17}$ cm^{-2}; contour B: $N(H)\sim 2.5\times10^{18}$ cm^{-2}; contour C: $N(H)\sim 5\times10^{18}$ cm^{-2}; contour D: $N(H)\sim 5\times10^{19}$ cm^{-2} (from Frisch and York, 1983, Astrophys. J., 271, L59).

the galactic poles. One can see from the figure that the contours of HI in the solar neighborhood asymmetrically surrounds the sun, with the 5×10^{18} cm^{-2} contour at < 15 pc in the Sco-Oph direction, but at 200 pc in the quadrant from $\ell = 180^{\circ}$ to $\ell = 270^{\circ}$. The sun is displaced from the center of an apparent hole in the neutral hydrogen. The contours map allow to locate a rough center for the hole at $\ell \sim 225^{\circ}$ $b \sim -15^{\circ}$ and r ~ 250 pc. This position falls remarkably close to the centroid of the Gould Belt main-sequence stars (see Section II.4).

Paresce (1984) analyzed the available data on the LISM (mainly interstellar absorption lines, in conjunction with EUV continuum absorption, polarization and color excess surveys), and translated all these results to neutral hydrogen column densities. In Fig. I.1.2 we report the contours of HI iso-column density given by the author. Strong density discontinuities are clearly observable at 100-150 pc towards $\ell \sim 180^{\circ}$ and towards $\ell \sim 270^{\circ}$, and a weaker discontinuity much closer to the sun towards $\ell \sim 60^{\circ}$. The data are consistent with a simple model that assumes the relatively pervasive presence of a tenuous ($n \sim 0.07$ cm^{-3}), possibly warm ($T \sim 10^3$-10^4 K) gas extending uniformly out to considerable distances from the sun in most directions. In the galactic longitude range $\ell \sim 200^{\circ}$ to $\ell \sim 270^{\circ}$ there is the only region manifestly clear of this material. These results are not in contrast with the HI 21 cm and soft X-ray surveys.

Recent very high-resolution and high signal-to-noise optical observations tend to support a quite complex structure of the LISM. Vidal-Madjar et al. (1986) claim the existence of two interstellar absorptions components within 15 pc of the sun in the direction of λSco. An analysis of the radial velocities imply that

Figure I.1.2

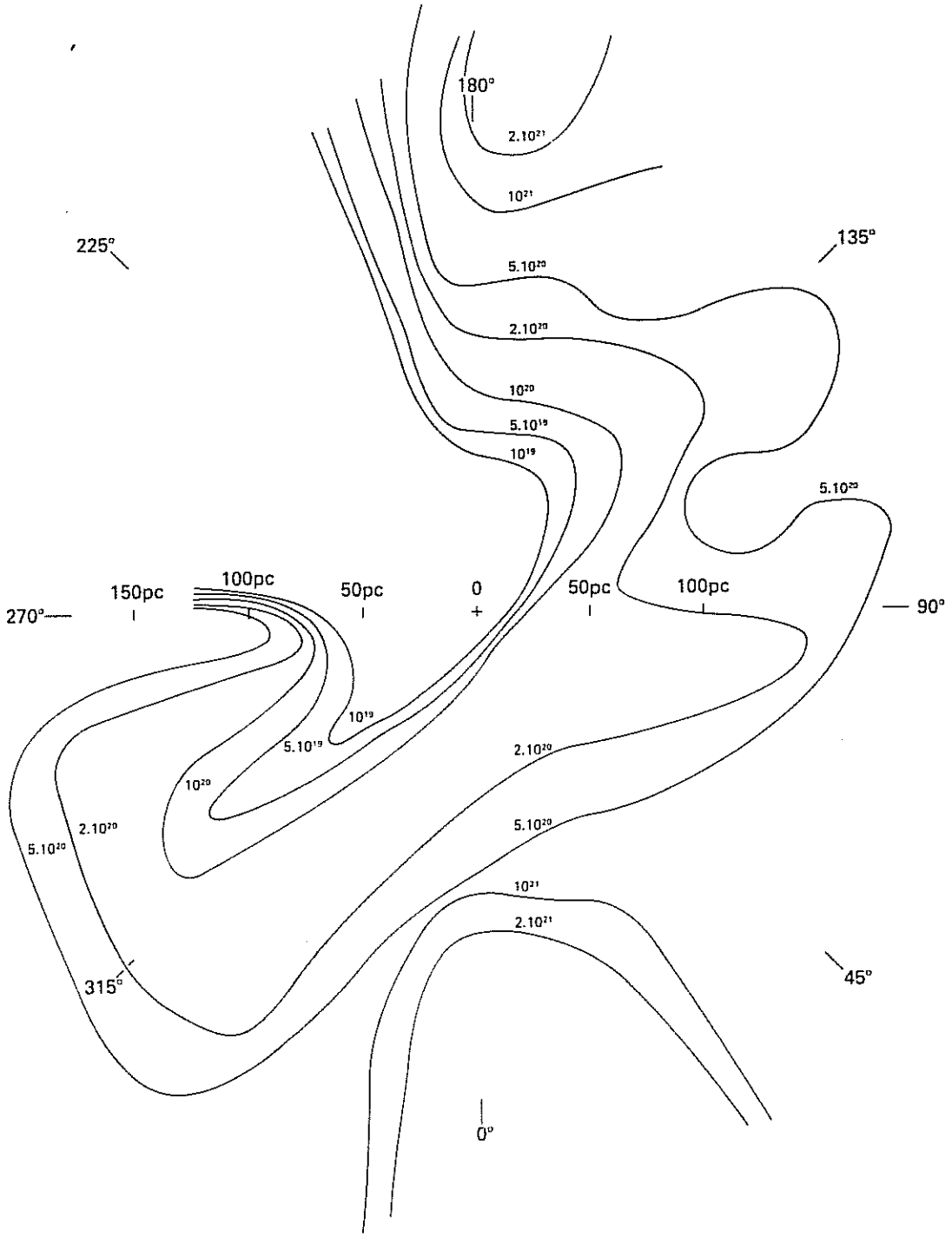

Estimated equal mean hydrogen column-density contours of the LISM in the galactic plane ($b < 30°$). The values of N(HI) are indicated on the corresponding contours. The position of the sun is at the origin of the coordinate system. (From Paresce, 1984, Astron. J., 89, 1022)

one of the component is moving according to the general direction found by Crutcher (1982), and the other according the direction found by backscattering measurements in the solar system (Section I.6). Ferlet et al. (1986) demonstrate the existence of at least three absorption components well separated in velocities towards the nearby (d = 5 pc) star α Aql. Two of these components have roughly the same column density, and are stronger than the other one. The radial velocity of one of the two strong components agrees with Crutcher's model of the LISM motion, while the radial velocity of the weak component agrees with the motion of the interstellar wind derived by backscattering measurements.

Observations of highly ionized species

During the last two decades UV astronomy has provided extensive evidence for the presence of highly ionized species in the ISM. Observations of OVI have been carried on with the Copernicus satellite since 1973. Jenkins and Meloy (1974) made the first systematic search for OVI absorption lines produced in the interstellar space, by means of the Copernicus spectrometer. They discovered the widespread presence of broad, shallow absorptions caused by OVI ions in the spectra of 32 early-type stars. Later Jenkins (1978a) completed this search, bringing to 72 the lines of sight showing OVI absorptions. Among the stars with positive detections, 17 lie at distances shorter than 200 pc, and 8 of them within 100 pc, so OVI is relevant for LISM investigations.

The fact that the observed absorptions are narrower than the broad OVI profiles produced by the atmospheres of hot stars, and the lack of an apparent correspondence between the radial velocity of the stars and those of the "narrow" OVI profiles argued againts a stellar origin.

The possibility that OVI is circumstellar is a more difficult issue to address. After a detailed discussion of the whole set of observed OVI absorptions, Jenkins (1978b) concluded that most of the OVI comes from truly interstellar material, but that some of the absorptions might be attributable to the evaporations zones within the very hot cavities created by the strong stellar winds produced by stars being observed (Appendix 3). An interesting result from Jenkins's (1978b) analysis, relevant to the LISM, is that the general

rate of increase of the OVI column density with distance $\underline{d}$, favors the existence of a positive intercept with $N(OVI) \sim 5 \times 10^{12}$ at $\underline{d}=0$. This offset could be interpreted as an excess resulting from the circumstellar bubbles around many of the stars, or as a contribution from a local concentration of hot gas in our neighborhood which has a disproportionate influence because all the lines of sight necessarily emanate from a single point instead of being randomly scattered about.

A detailed statistical analysis of the observed OVI absorptions (Jenkins 1978c) brought the following results. Fluctuations in column densities over various lines of sight suggest the existence of six hot gas regions per kiloparsec, randomly distributed in space, each with an OVI column density of about 10^{13} cm^{-2}. The statistics of radial velocity centroids and line widths support the interpretation of distinct domains. Each region has an internal velocity dispersion consistent with a Doppler broadening of a plasma at $T > 2 \times 10^5$ K, near the characteristic temperature for a maximum concentration of OVI in collisional equilibrium.

The OVI bearing regions show a velocity dispersion of 26 km/s, markedly higher than for ordinary interstellar clouds. This is perhaps not surprising if the gas is produced by shocks from supernovae (Cox and Smith 1974) or disturbances generated by high-velocity interstellar clouds. In this case stabilization by normal interstellar material must have occurred, since the dispersion in radial velocity is much smaller than that expected from the shock speed of $\sim$ 150 km/s needed to heat the gas to the temperatures for collisionally ionizing oxygen to +5 ($T \sim 3 \times 10^5$ K). A completely different viewpoint is that the OVI is produced within conductive

interfaces between dense clouds and a much hotter medium, as in the theory of McKee and Ostriker (Section II.1).

Jenkins (1978c) concluded also that the filling factor of the OVI-bearing regions must be less than 20%, provided most of interstellar space is filled with the gas responsible for the reddening of the observed stars and not some other phase at low density.

The regions of lower temperatures producing OVI should also be detected in other highly ionized atoms, most particularly CIV, SiIV and NV, which have resonance lines in the UV and which form in gas at only slightly lower temperatures. Surveys of CIV and SiIV have been carried out in a large number of stars with the IUE satellite. The interstellar nature of CIV and SiIV detected in the halo is firmly established (Pettini and West 1982). CIV and SiIV narrow absorptions have been detected in spectra of extragalactic sources at the position expected for a co-rotating halo and at rest in a number of halo stars with high radial velocities.

The situation in the disk is more confused and there is no clear-cut evidence for pervasive interstellar CIV and SiIV gas. Many authors have suggested that CIV and SiIV could be produced through photoionization by stellar ultraviolet photons in the HII regions surrounding the stars (Black et al. 1980, Cowie et al. 1981, Smith et al. 1980). On the other hand, it has been objected that no correlation between column densities of CIV and SiIV with the stellar effective temperature appears from the data (Jenkins 1981), as is expected in the case of stellar photoionization.

Molaro et al. (1984) have detected narrow interstellar-like CIV and SiIV absorptions in the spectra of four rapidly rotating late-type B stars within 200 pc of the sun. Because the effective temperature of these stars is low (Teff $\sim$ 12,000 K), it is not possible for the CIV and SiIV to be formed by photoionization from stellar UV flux. Molaro et al. (1986) have enlarged the sample of targets under investigation to a total of six nearby late-type B fast rotators. They conclude that it is not yet clear whether the absorptions originate in the surroundings of the stars or in the diffuse ISM: the FWHM's of the lines point to an interstellar origin, but nearly all the stars in which CIV and SiIV are detected are Be and the absorptions could in fact be associated with the extended envelope around the stars.

References

Anderson,R., Weiler,E.J., 1978, Astrophys. J., 224, 143.

Black,J.H., Dupree,A.K., Hartmann,L.W., Raymond,J.C.: 1980, Astrophys. J., 239, 502.

Bruhweiler,F.C., 1982, NASA CP-2238, p. 125.

Bruhweiler,F.C., Oegerle,W., Weiler,E., Stencel,R., Kondo,Y., 1984, IAU Coll. 81, NASA CP-2345, p. 64.

Cowie,L.L., Taylor,W., York,D.G.: 1981, Astrophys. J., 248, 528.

Crutcher,R.M., 1982, Astrophys. J., 254, 82.

Ferlet,R., Lallement,R., Vidal-Madjar,A.: 1986, Astron. Astrophys., 163, 204.

Frisch,P.C., York,D.G.: 1983, Astrophys. J., 271, L59.

Jenkins,E.B., Meloy,D.A.: 1974, Astrophys. J., 193, L121.

Jenkins,E.B.: 1978a, Astrophys. J., 219, 845.

Jenkins,E.B.: 1978b, Comments Astr., 7, 121.

Jenkins,E.B.: 1978c, Astrophys. J., 220, 107.

Jenkins,E.B.: 1981, "The Universe at Ultraviolet Wavelengths", ed. R.D.Chapman, Greenbelt, NASA CP-2171, p. 241.

Jenkins,E.B.: 1984, IAU Coll. 81, "Local Interstellar Medium", NASA CP-2345, p. 155.

Molaro,P., Beckman,J.E., Franco,M.L., Morossi,C., Ramella,M.: 1984, IAU Coll. 81, "Local Interstellar Medium", NASA CP-2345, p. 185.

Molaro,P., Vladilo,G., Beckman,J.E.: 1986, "New Insights in Astrophysics", London, July 1986, ESA SP-263, p. 679.

Murthy,J., Henry,R.C., Moos,H.W., Landsman,W.B., Linsky,J.L., Vidal-Madjar,A., Gry,C.: 1986, Astrophys. J., submitted.

McClintock,W., Henry,R.C., Linsky,J.L., Moos,H.W., 1978, Astrophys. J., 225, 465.

Paresce,F., 1984a, IAU Coll. 81, NASA CP-2345, p. 169.

Paresce,F., 1984b, Astron. J., 89, 1022.

Pettini,M., West,K.A.: 1982, Astrophys. J., 260, 561.

Smith,L.J., Willis,A.J., Wilson,R.: 1980, M.N.R.A.S., 191, 339.

Stokes,G.M.: 1978, Astrophys. J. Suppl., 36, 115.

Vidal-Madjar,A., Ferlet,R., Gry,C., Lallement,R., 1986, Astron. Astrophys., 155, 407.

York,D.G., Frisch,P.C., 1984, IAU Coll. 81, NASA CP-2345, p. 51.

2. OPTICAL EMISSION LINES

One way to investigate the physical state of the interstellar ionized gas is to study the emission lines of the type of those produced in HII regions (see e.g. Osterbrock 1974). The use of specially dedicated instruments has allowed to detect faint optical emission lines spatially diffuse. Numerous observations have been made of the H_α emission using a Fabry-Perot spectrometer (Reynolds et al. 1974). The emission is associated both spatially and kinematically with the large-scale galactic structure within a few kiloparsecs of the sun and appears to be produced by an ionized component of the interstellar medium that is outside the bright, localized HII regions.

The H_α background near the galactic equator is not directly relevant for LISM studies, since it appears to originate from gas distributed out to 3 kpc or more from the sun (see Reynolds 1984). On the other hand, observations at high galactic latitudes sample interstellar material that is more local. The H_α emission intensity decreases with increasing latitude, consistently with a disk-like distribution of the emitting gas, although the scatter in intensities at any given latitude suggests that the distribution is not uniform. The radius of the region surrounding the sun within which the H_α emission at a given latitude originates depends upon the scale height of the emitting gas. Pulsar observations indicate a scale height H =

500-1000 pc for the density of free electrons (Readhead and Duffet-Smith 1975). These electrons appear to be clearly associated with the H_α emitting regions (Reynolds 1984a). If the electron density decreases exponentially with increasing height z above the galactic plane, then the H_α emission from this gas would originate from a region with a scale height of H/2, since the line emissivity is proportional to the square of the electron density. This suggests that the emission at galactic latitudes $|b| > 60^\circ-70^\circ$ is from gas primarily located within a cylinder of radius 150 pc centered on the sun.

Although interstellar grains may scatter H_α photons from bright HII regions located near the galactic plane, the observations towards high latitude reflection nebulae indicate that the intensity of this scattered component is small compared to the total background intensity that is observed. Additional strong evidence that such scattered light is not a dominant source of background emission has been provided by the discovery that the [SII]6716/H intensity ratios in the diffuse background are approximately 3-4 times higher than the ratios found in the classical HII regions.

The detection of the collisionally excited [NII]6583 and [SII]6716 emission in the galactic background places a lower limit of about 3000 K on the temperature of the emitting gas. If the HII, NII and SII ions are well mixed within the ionized regions, then the observed widths of the lines indicate a temperature $T \sim 10^4$ K. The absence of detectable [OI]6300 and [NI]5200 suggests a high fractional ionization of hydrogen ($HII/H \sim 0.75$). A typical electron density of 0.1-0.2 cm^{-3} within an ionized region has been derived from a

comparison of emission measures and pulsar dispersion measures (Reynolds 1977). This analysis also indicates that the ionized component occupies 10-30% of the interstellar volume. The observations of interplanetary hydrogen and helium (Section I.6) confirm that this component is an important constituent of the LISM.

References

Osterbrock,D.E.: 1974, Astrophysics of Gaseous Nebulae, Freeman and Company.

Readhead,A.C.S., Duffet-Smith,P.J.: 1975, Astron. Astrophys., 42, 151.

Reynolds,R.J.: 1977, Astrophys. J., 216, 433.

Reynolds,R.J.: 1984, IAU Coll. 81, "Local Interstellar Medium", NASA CP-2345, p. 97.

Reynolds,R.J.: 1984a, Astrophys. J., July 1.

Reynolds,R.J., Roesler,F.L., Scherb,F.: 1973, Astrophys. J., 179, 651.

Reynolds,R.J., Roesler,F.L., Scherb,F.: 1977, Astrophys. J., 211, 115.

3. RADIO OBSERVATIONS

It is difficult to distinguish the neutral hydrogen component of the LISM by means of HI 21 cm observations, since the weak emission from local gas may be blended with stronger emission from more distant gas. An independent knowledge of the expected velocity of the LISM, such as that derived by Crutcher (1982) and discussed in Section I.1, allows to separate the local gas component from more distant components with different radial velocities, provided we are not looking at directions nearly perpendicular to the LISM velocity vector. So upwind and downwind directions should be more favorable to distinguish local 21 cm emissions. The downwind direction (i.e., roughly the galactic anticenter) is less favorable than the upwind direction because gas within 1 kpc of the sun generally has positive velocity, so the greatest separation between local and distant emission occurs in the upwind direction (i.e., roughly the galactic center).

Crutcher (1982) compared the 21 cm observations of Sancisi and van Woerden (1970) with Hobb's (1971) optical and radio observations and concluded that there is evidence for a HI cloud moving at the same velocity of the LISM, closer than 170 pc from the sun, from the Sco-Oph direction.

After including a discussion on the HI observations from Colomb et al. (1980), Crutcher concluded that the neutral hydrogen out of the

galactic plane in the upwind hemisphere of the sky is moving at the same velocity found from his analysis of absorption lines towards nearby stars. Part of this HI is moving at more positive velocities, but this fact might be ascribed to emission from a more distant gas.

Another way to identify local structures of HI, is to study features covering a large angular extent on the sky. The most relevant structure revealed by the 21 cm observations is a conspicuous set of arching concentric filaments extending more than 80° on either side of $\ell = 330°$. The arching pattern is also shown by the position angles of optical polarization vectors of nearby stars: the magnetic fields that orient the polarization-producing grains lie along the elongated space-density structures that we observe as HI filaments. The center of curvature determined by the position-angles of optical polarization is $\ell = 331°$, $b = +14°$. Distances of stars whose light is polarized by the aligned grains in the arching filaments indicate that the structure extends over the distance range from 20 to 400 pc (Weaver 1979).

Also non-thermal radio emission observations are important for understanding the LISM. The existence of ridges of enhanced continuum emission going to high latitudes has been known since the earliest days of radio astronomy. Berkhuijsen et al. (1971) adopted the name "loop" to indicate a combination of features which form a small circle in the sky. In Table I.3.1 are reported the geometrical parameters of the galactic radio loops, which are traced in galactic coordinates in Fig. I.3.1. It is clear that the center of Loop I is remarkably coincident with the center of the HI structure described in the

Table I.3.1

The small circle parameters of the galactic loops

Object	l (centre)	b (centre)	Diameter	R. M. S. Deviation	Arc Length
Loop I	329° ± 1°5	+17°5 ± 3°	116° ± 4°	0°9	155°
Loop II	100° ± 2°	−32°5 ± 3°	91° ± 4°	1°1	150°
Loop III	124° ± 2°	+15°5 ± 3°	65° ± 3°	1°7	180°
Loop IV	315° ± 3°	+48°5 ± 1°	39°5 ± 2°	0°8	190°

Figure I.3.1

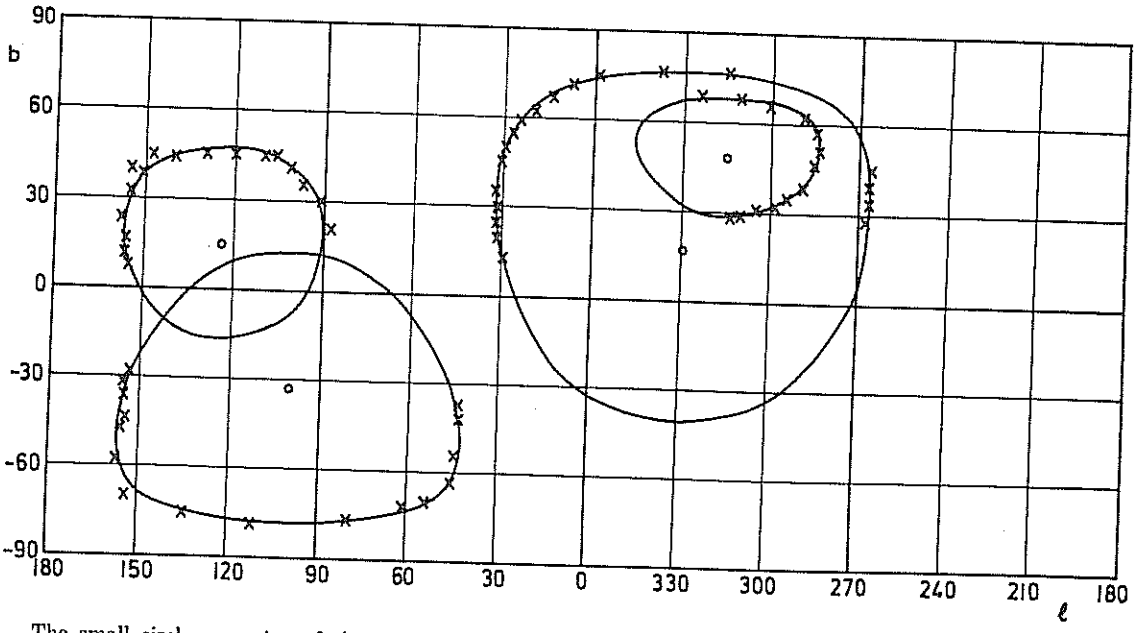

The small circle geometry of the Galactic loops. The crosses mark measured ridge positions used to compute the small circles

preceding paragraph. Indeed, the large shell visible in synchrotron radiation overlaps the arching HI filaments. The intense continuum ridge which runs to high positive latitudes around $\ell = 30^{\circ}$ is called North Polar Spur and is clearly a part of Loop I. Berkhuijsen et al. (1971) showed that there is a correlation between the galactic loops and neutral hydrogen, and that the supernova remnant hypothesis seems consistent with the geometry of the loops. The linear diameter and average surface brightness at 1 GHz of the galactic loops confirm that they are old ($\sim 10^{6}$ years) supernova remnants (Berkhuijsen 1973).

The angular diameter of Loop I is about 120°, which suggests that its near side is very close to the sun. Berkhuijsen (1973) suggested that the center of this shell is about 130 ± 75 pc from the sun, which would place most part of the spherical shell well inside the LISM, with the nearest side at 15 ± 75 pc from the sun. It is important to stress that the center of Loop I roughly coincides with the center of the Sco-Cen OB association ($\ell = 330^{\circ}$, $b = +18^{\circ}$), which is $\sim$ 170 pc distant and which seems to be responsible for the streaming of the LISM gas (Weaver 1979).

References

Berkhuijsen,E.M.: 1973, Astron. Astrophys., 24, 123.

Berkhuijsen,E.M., Haslam,C.G.T., Salter,C.J.: 1971, Astron. Astrophys., 14, 252.

Colomb,F.R., Poppel,W.G.L., Heiles,C.: 1980, Astron. Astrophys. Suppl., 40, 47.

Crutcher,R.M.: 1982, Astrophys. J., 254, 82.

Sancisi,R., van Woerden,H.: 1970, Astron. Astrophys., 5, 135.

Weaver,H.: 1979, in The Large Scale Characteristics of the Galaxy, IAU Symp. 84, ed. W.B.Burton (Dordrecht:Reidel), p. 295.

4. SOFT X-RAY OBSERVATIONS

The soft X-ray diffuse background provides unique information about the hot phases of the ISM, the galactic halo, and the intergalactic gas. The Wisconsin group (see McCammon et al. 1983) began in 1972 a program to map the distribution of the X-ray diffuse background over the entire sky as a function of energy in the 0.1 - 10 keV range. This survey was carried out with proportional counters having a 6.5 degrees FWHM field of view covering seven energy bands.

The results obtained with the so called B and C bands are the most relevant for LISM studies. The B band responds from approximately 130 eV to the boron K-shell absorption edge at 188 eV. The C band extends from about 160 eV to the carbon cutoff at 284 eV. In Figs. I.4.1 and I.4.2 are shown the intensity maps in galactic coordinates for the B and C bands respectively. The B and C band maps appear very similar, with the exception of a northern emisphere feature near $\ell = 30^{\circ}$ that has been identified with the North Polar Spur (see also Fig. I.3.1). It is important to note that there is a finite flux in the galactic plane, which is approximately the same for all longitudes. In Fig. I.4.3 is shown for comparison the 21cm HI column density map given by Cleary et al. (1979). Both of the soft X-rays maps show a general increase in count rate towards the galactic poles, particularly in the northern emisphere. Comparison with the N(HI) map shows a striking anticorrelation between X-ray intensity and

B Band

Fig. I.4.1

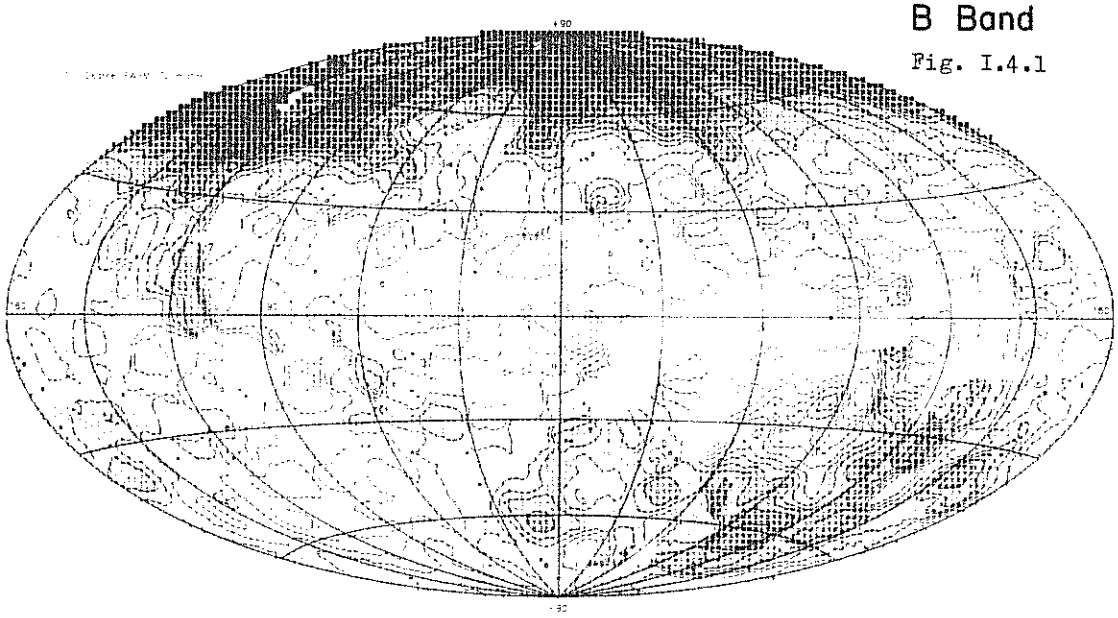

C Band

Fig. I.4.2

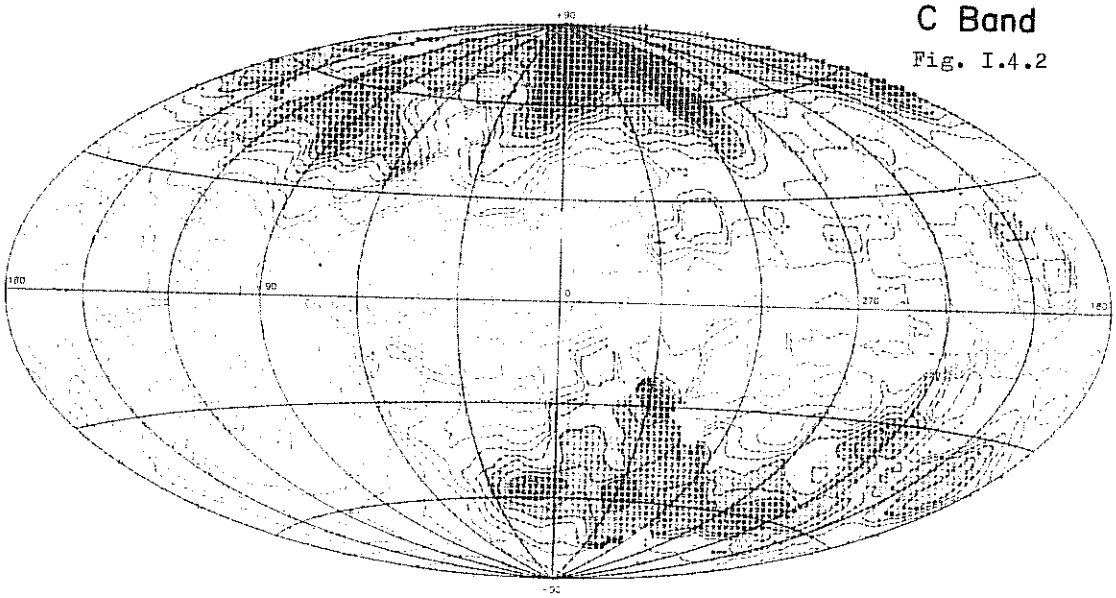

N_H

Fig. I.4.3

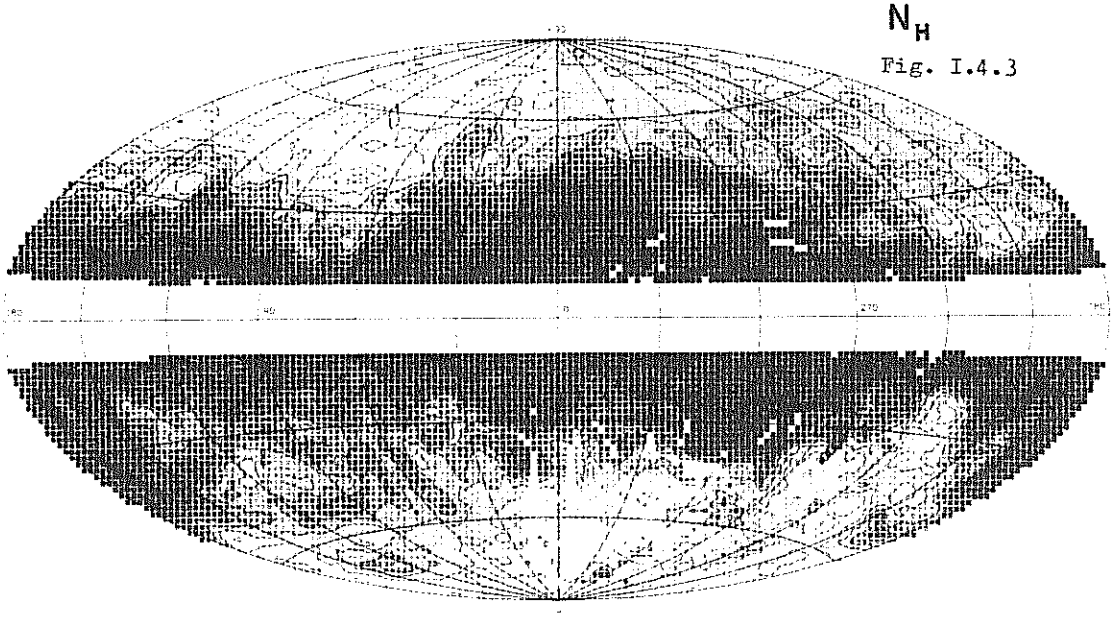

HI column density.

If discrete sources in the galactic disk provided the majority of the observed flux, limits on the small-scale fluctuations of the background would require a space density at least equal to that of the most common stars. Stars themselves can provide at most $\sim$ 3% of the flux in the range 0.15 to 0.28 keV (Rosner et al. 1981). These arguments show that the source of the soft X-ray background must be truly spatially diffuse.

Now, let us show that nonthermal diffuse mechanisms cannot be responsible for the observed soft X-ray flux (Williamson et al. 1974). While a gross extrapolation of the galactic radio spectrum to X-ray energies yields intensities close to those measured by Williamson et al. (1974), a synchrotron mechanism for the X-ray production seems most unlikely. In the first place, the spectral index of the X-radiation is much larger than the radio index. Second, the lifetime of the 3.5×10^{13} eV electrons required to produce 0.25 keV X-rays in a 3×10^{-6} gauss field is less than 10^4 years due to inverse Compton and synchrotron losses. An inverse Compton origin of the soft X-rays seems equally hard to accomodate. Electrons of $\sim$ 250 MeV can scatter the 3 K radiation into the very soft X-ray region, but the required number of energetic electrons is unreasonably large. Their energy density would be $\sim 10^2$ eV cm^{-3}, and the flux of high-energy gamma rays (E > 100 Mev) produced by bremsstrahlung of these electrons on the interstellar gas would be $\sim 10^3$ times that measured. Electrons of $\sim$ 6 MeV can scatter starlight into the very soft X-ray region. But the energy density of these electrons would be $\sim$ 1500 eV cm^{-3}, and there would result an interstellar ionization rate $\sim$ 250 times the upper

limit set by Field et al. (1969).

The above arguments leave diffuse thermal emission from a gas at $T \sim 10^6$ K as the probable source of the soft X-ray background. The existence of such gas was suggested long ago (Spitzer 1956), and the obervations of interstellar OVI (Section I.1) now provide solid evidence for the existence of gas at only slightly lower temperatures. Let us now discuss the problem of the location of the emitting gas.

Absorption model

If the emitting material were located beyond the galactic neutral gas, then absorption by this cool interstellar material would provide a natural explanation for the observed anticorrelation of X-ray intensity and neutral hydrogen column density. A truly extragalactic origin for the B and C bands seems unlikely due to lack of apparent absorption by the Small Magellanic Cloud (McCammon et al. 1976) and the Large Magellanic Cloud (Long et al. 1976), so the absorption model requires a galactic origin for the emitting gas.

A hot galactic halo or corona has a sound theoretical basis (Spitzer 1956, Chevalier and Oegerle 1979), and there is observational evidence of highly ionized material above the plane (Savage and de Boer 1981). Absorption of the radiation coming from hot gas in a galactic corona is therefore an attractive possibility for explaining the observed anticorrelation of X-ray intensity and neutral hydrogen column density.

There are however problems with the model of an absorbed coronal origin for the B and C bands. McCammon et al. (1983) examined the

general X-ray intensity versus HI column density to quantitatively test this model as an explanation of the observed anticorrelation. The following difficulties are apparent: (1) in spite of the very short mean free path of the soft X-ray photons, there is residual flux in the galactic plane which is about 30% of the observed maximum intensity. This problem is resolved by including in the model an isotropic local (unabsorbed) X-ray emission component (this component accounts for more than half the total B and C band flux). (2) There is more scatter in the HI column density versus X-ray intensity relation than is consistent with a simple absorption model. The problem may be with the 21 cm HI data (radio beam side lobes contributions). Another possibility is that the local X-ray component is not isotropic. (3) The experiments of McCammon et al. (1976) and Long et al. (1976) designed to test for X-ray absorption by the Magellanic Clouds, also detected no absorption by galactic gas. (4) Quantitatively, the X-ray intensity variations with changing HI column densities are much smaller than predicted by the atomic cross sections of Brown and Gould (1970). (5) The X-ray intensity variations do not show the large energy dependence predicted by the photoelectric absorption.

A possible explanation for the anomalous absorption behaviour is clumping of the absorbing gas. If the interstellar gas were clumped on angular scales smaller than the X-ray beam into randomly distributed clouds, then the effective X-ray cross section would depend on the thickness (column density) of the clouds. If all the interstellar material were clumped in clouds of average thickness $2\text{-}3\times10^{20}$ cm^{-2} the effective cross sections of the B and C bands would

be in good agreement with the observed ones in the absorption model. However 21 cm observations put severe constraints on the angular size of the clouds and are not in agreement with a clumping at this level.

Displacement model

Owing to the difficulties of the absorption model another way of explaining the observed anticorrelation has been suggested (Sanders et al. 1977): since a local emission component seems required in any case, it could provide essentially all the observed flux in the B and C bands. Assuming that the source is thermal radiation from a diffuse plasma, the required temperature is near 10^6 K. Pressure arguments then favour an extent of roughly 100 pc, in agreement with optical and UV interstellar absorption results, which show a region of anomalously low density of similar extent around the sun (Section I.1). This is comparable to the scale height of the HI distribution, so the hot material displaces a significant column density of neutral gas. If spatial features in the B and C bands are caused by variations in the extent of the emitting region, one would expect them to be anticorrelated with HI column density due to corresponding variations in the amount of neutral gas displaced. Unfortunately, this displacement model makes few quantitative predictions that can be tested without knowing the three-dimensional distribution of cool interstellar material in the solar neighbourhood. One definite prediction which agrees well with observations is that the correlation with HI should be entirely energy-independent. Extension of the X-ray observations to longer wavelengths would also be very helpful; if the similarity in spatial distribution seen in the C and B bands persists at lower energies, it will be a stronger argument in favor of a local

origin for all of these X-rays.

The X-ray results indicate that the emission measure of the hot bubble is of the order EM ~ $1\text{-}3\times10^{-3}$ cm^{-6} pc, if there is virtually no absorption. Assuming a mean free path of 100 pc along the bubble, and a temperature $T \sim 10^6$ K, one must conclude that the thermal pressure of the gas is $P/k \sim 10^4$ K cm^{-3}. This pressure exceeds by a substantial margin the general ISM value of 2000-3000 K cm^{-3} (Spitzer 1978).

Soft X-rays emission lines

An independent proof of the thermal origin of the Soft X-ray emission is given by the observation of emission lines of elements in very high stages of ionization. Inoue et al. (1979) detected an emission peak at about 0.57 keV identified as O VII. The spectrum is in agreement with that of thermal emission from tenuous plasma of a temperature $T \sim 1.4\times10^6$ K. Rocchia et al. (1984) confirm the thermal nature of the diffuse emission by the observation of C V, C VI and O VII. Assuming normal abundances and ionization equilibrium, the temperature of the emission from the local hot gas was determined to be 1.14×10^6 with an accuracy better than 10% at the 90% confidence level. Evidence was given for the existence of a weak component at a higher temperature, possibly produced by a hot galactic halo.

References

Brown,R.L., Gould,R.J.: 1970, Phys. Rev. D, 1, 2252.

Chevalier,R.A., Oegerle,W.R.: 1979, Astrophys. J., 227, 398.

Cleary,M.N., Heiles,C., Haslam,C.G.T.: 1979, Astron. Astrophys. Suppl., 36, 95.

Field,G.B., Goldsmith,D.W., Habing,H.J., 1969, Astrophys. J., 155, L149.

Kraushaar,W.L.: 1973, in Gamma Ray Astrophysics, eds. Stecker and Trombka, NASA SP-339, p.3.

Inoue,H., Koyama,K., Matsuoka,M., Ohashi,T., Tanaka,Y.: 1979, Astrophys. J., 227, L85.

Long,K.S., Agrawal,P.C., Garmire,G.P.: 1976, Astrophys. J., 206, 411.

McCammon,D., Meyer,S.S., Sanders,W.T., Williamson,F.O.: 1976, Astrophys. J., 209, 46.

McCammon,D., Burrows,D.N., Sanders,W.T., Kraushaar,W.L.: 1983, Astrophys. J., 269, 107.

Rocchia,R., Arnaud,M., Blondel,C., Cheron,C., Christy,J.C., Rothenflug,R., Schnopper,H.W., Delvaille,J.P.: 1984, Astron. Astrophys., 130, 53.

Rosner,R., Avni,Y., Bookbinder,J., Giacconi,R., Golub,L., Harnden,F.R., Maxson,C.W., Topka,K., Vaiana,G.S.: 1981, Astrophys. J., 249, L5.

Sanders,W.T., Kraushaar,W.L., Nousek,J.A., Fried,P.M.: 1977, Astrophys. J., 217, L87.

Savage,B.D., deBoer,K.S.: 1981, Astrophys. J., 243, 460.

Spitzer,L.: 1956, Astrophys. J., 124, 20.

Spitzer, L., Jr., 1978, Physical Processes in the Interstellar Medium, John Wiley and Sons, Inc..

Williamson,F.O., Sanders,W.T., Kraushaar,W.L., McCammon,D., Borken,R., Bunner,A.N.: 1974, Astrophys. J., 193, L133.

5. INFRARED AND MILLIMETRIC OBSERVATIONS

Among the unexpected results from the Infrared Astronomical Satellite (IRAS) was the discovery of large-scale, extended filamentary emissions at 60 and 100 microns, described as "infrared cirrus" by Low et al. (1984). These highly structured extended sources superposed on a continuum IR background were originally supposed to be originated either in the interplanetary medium, the outer solar system, or the interstellar medium. Three classes of phenomena were identified by Low et al. (1984): (1) thermal emission at 60 or 100 microns, or both, positionally associated with the strongest concentrations of gas and dust at very high galactic latitudes as indicated by HI studies (Burnstein and Heiles 1982); (2) large features associated with the ecliptic; (3) emissions poorly correlated with known interstellar gas clouds, possibly new parts of the outer solar system or new structures within the interstellar medium. Indeed, much of the structure seen in the 100 microns scans belongs to the last category. This dust emission could, perhaps, be associated with HI at anomalous velocities, or with clouds with molecular rather than atomic hydrogen, or with cold material in the outer solar system.

Concurrent with the discovery of the IRAS cirrus, Blitz et al. (1984) reported the detection of a large number of high galactic latitude ($|b| > 25^\circ$) CO molecular clouds not previously cataloged.

Magnani et al. (1985) published maps of these molecular clouds, which show a range of morphologies with extents sometimes exceeding 10°. The cloud-to-cloud velocity dispersion of these objects is 5.6 km/s, which implies an expectation value $\langle z \rangle \sim 60$ pc for the height of a cloud above the galactic plane. The expectation value $\langle d \rangle$ for the distance to a cloud is then $\langle d \rangle = \langle z \rangle \cos b$, and a mean value $\langle d \rangle \sim 100$ pc is found for the clouds of Magnani et al. (1985). Using this distance for the clouds one obtains that their average sizes and masses are of 1.7 pc and 40 $M_{\odot}$. Many of the clouds have an internal velocity dispersion which is an order of magnitude greater than the velocity dispersion obtained by the virial theorem. This implies that they are not gravitationally bound. If so, because the clouds are so small, their ages are less than the crossing time for the clumps: $< 10^{6}$ years. These clouds appear to be extraordinarily young and may represent the earliest stages of molecular material condensing from the ISM.

On the basis of the large angular sizes of the CO clouds Blitz et al. (1984) suggested that the IRAS cirrus could be emission from high latitude molecular clouds. Weiland et al. (1986) showed that for each CO cloud mapped by Magnani et al. (1985) the IRAS 100 micron image shows cirrus of similar structure. In particular there is close correspondence between the 100 microns emissions peaks and the CO intensity peaks. So it is possible to adopt for these cirrus clouds the average properties of the ensemble of high latitude molecular clouds reported by Magnani et al. (1985).

Hobbs et al. (1986), observing the NaI D IS lines towards 9 A and F stars, have shown that one of the high latitude CO clouds lies at $\sim$

65 pc, within the local region filled primarily by very hot, low-density gas. This, together with the extended angular size of many CO clouds, gives more weight to the statistical arguments which put the clouds in the solar neighbourhood.

Another interesting result is the existence of clouds containing HI but not H_2, as indicated by the non detection of CO in some cirrus features identified by Low et al. (1984). Two kinds of clouds appear to exist: predominantly atomic and predominantly molecular. A mechanism must be identified for inducing transition between these two kinds of clouds.

References

Blitz,L., Magnani,L., Mundy,L.: 1984, Astrophys. J. , 282, L9.

Burstein,D., Heiles,C.: 1982, Astron. J., 87, 1165.

Hobbs,L.M., Blitz,L., Magnani,L.: 1986, Astrophys. J., 306, L109.

Low,F.J., Beintema,D.A., Gautier,T.N., Gillett,F.C., Beichman,C.A., Neugebauer,G., Young,E., Aumann,H.H., Boggess,N., Emerson,J.P., Habing,H.J., Hauser,M.G., Houck,J.R., Rowan-Robinson,M., Soifer,B.T., Walker,R.G., Wesselius,P.R.: 1984, Astrophys. J., 278, L19.

Magnani,L., Blitz,L., Mundy,L.: 1985, Astrophys. J., 295, 402.

Weiland,J.L., Blitz,L., Dwek,E., Hauser,M.G., Magnani,L., Rickard,L.J.: 1986, Astrophys. J., 306, L101.

6. INTERPLANETARY MEASUREMENTS

The interstellar matter moving with respect to the solar system enters the gravitational field of the sun and directly interacts with the solar wind and the solar EUV flux. Well outside the outer boundary of the solar system, a "collisionless shock" forms as a consequence of interactions between the charged particles in the inflowing interstellar material and those of the outflowing solar wind. Immediately inside the shock front lies a turbulent shell of plasma, called the heliospheric interface. The inner part of this interface is called the heliosphere. The neutral interstellar medium is able to penetrate the heliosphere and to reach the solar system before being ionized. Thus, the solar system is swept by an "interstellar wind" which can be detected by resonance scattering emission of HI (Lyα) and HeI (λ584Å) atoms illuminated by the sun.

From the intensity distribution of the backscattered radiation in the solar system, one can derive the density of H and He in the LISM and the direction of the motion $\underline{V}_w$ between the sun and the LISM. The velocity module V_w and the LISM temperature are more adequately found from a measurement of the Lyα line shape, which is an image of the velocity distribution of H atoms.

Bertaux (1984) gives a summary of results of observations within the solar system by means of the Prognoz satellite. The velocity V_w is found to be 20 $\pm$ 1 km/s in a direction quite different from the

Apex one: this means that the LISM is moving also in respect to the LSR. The LISM motion in the LSR has a velocity of 16 km/s from the direction $\ell = 304°$, $b = -4°$. This direction is significantly different from the direction ($\ell = 345°$, $b = -10°$) found by interstellar absorption lines on stars within ~ 100 pc (see Section I.1). According to Bertaux, the temperature of the LISM is T = 8000 ± 1000 K, the H density n(H) ~ 0.04 to 0.06 cm^{-3}, and the He density n(He) ~ 0.015 to 0.020 cm^{-3}.

It is important to note that the interstellar He, which cannot be observed from stellar measurements because its resonance wavelength falls in the EUV, has been detected and mapped in the solar system by means of backscattering measurements. The comparative study of H and He raises several questions, in particular about the ionization degree of the LISM and the interaction between the solar wind and the interstellar plasma.

The low [H/He] ratio measured with backscattering ([H/He] ~ 2 to 4), in respect to the cosmic value ([H/He] ~ 10), would imply that a substantial part of the hydrogen is ionized, assuming that He is not significantly ionized. Nevertheless, there are at least two difficulties for deriving the ionization state of the LISM from HI and HeI measurements in the solar system:

(1) nothing precludes He from being partially ionized. In fact, it is not excluded that the ionization state of the LISM is determined by a progressive recombination following a sudden ionization due, for example, to the blast wave of a supernova explosion (Sections II.2 and II.3).

(2) Some HI atoms are perhaps lost by charge exchange with interstellar protons at the heliospheric interface. It has been suggested that this process could ionize up to 50% of the inflowing interstellar hydrogen and thus significantly affect the HI density derived from the backscattered Lyα within the solar system (Ripken and Fahr 1983). As a consequence, the hydrogen temperature should be increased relative to that of helium. The opposite temperature relationship actually appears to be observed, however, except towards the downwind direction, where the data suggest that T_H (downwind) > T_{He} (downwind) > T_H (upwind) (Bertaux et al. 1985). Bertaux (1984) has argued that the apparent increase in the hydrogen and helium temperatures downwind are a strong indication that deviations from the model are more related to an interaction near the sun than near the heliospheric boundary and thus the parameters derived from upwind data accurately characterize the conditions in the LISM around the sun.

Chassefiere et al. (1986) discuss the results of the backscattering observations by means of the Venera 11 and 12 spacecrafts, distinguishing two cases: (1) the heliospheric interface is "transparent", i.e. the HI density is not affected by charge exchange reactions; (2) the heliospheric interface is "semi-transparent", i.e. there is a partial extintion of neutral hydrogen at the plasma interface. They conclude that there are 3 possible ionization states of the nearby ISM consistent with their measurements: (1) a low H density ($\sim$ 0.05 to 0.15 cm^{-3}) and a weak fractional ionization ($x < 0.1$) in the case of a semi-transparent heliospheric interface; (2) the same low H density and a greater ionization fraction ($x \sim 0.3$) in the case of a transparent

heliospheric interface and ionization equilibrium; (3) a high H density ($\lesssim$ 1 cm^{-3}) and a strong fractional ionization in the case of a transparent heliospheric interface and a non-equilibrium ionization due to a supernova explosion between 10^5 and 10^6 years ago.

References

Bertaux,J.L.,: 1984, IAU Coll. 81, "Local Interstellar Medium", NASA CP-2345, p. 3.

Bertaux,J.L., Lallement,R., Kurt,V.G., Mironova,E.N.: 1985, Astron. Astrophys., 150, 1.

Chassefiere,E., Bertaux,J.L., Lallement,R., Kurt,V.G.: 1986, Astron. Astrophys. 160, 229.

Ripken,A.W., Fahr,A.J.: 1983, Astron. Astrophys., 122, 181.

SECOND PART

MODELS OF THE LISM

1. THE GENERAL INTERSTELLAR MEDIUM

It would be impossible to introduce models on the LISM without a brief description of the theories on the general interstellar medium. Some details on physical processes relevant for these theories are treated separately in the Appendices.

Before the observations put in evidence the existence of the hot interstellar regions, a 2-phase model of the ISM was proposed by Field, Goldsmith and Habing (1969). In this model a steady-state mechanism (cosmic-ray ionization) heats the cold ($T < 100$ K) clouds and produces a warm ($T \sim 10^4$ K) "intercloud medium" in pressure equilibrium with the clouds; the intercloud medium occupies most of interstellar space. For a given value of the cosmic-ray energy density, and a cooling function due to collisional excitations in a gas of cosmic abundance (Appendix 1), the models give the electron density, n_e, and the equilibrium temperature, T, as functions of the total gas density, n. In Fig. II.1.1 we show the resulting thermal pressure, $P/k = (n_e+n)\ T$, as a function of the gas density, n. Three phases for the gas are indicated: F ($T \sim 10^4$ K), G ($T \sim 5000$ K), and H ($T \sim 100$ K). All three can coexist in pressure equilibrium, but phase G is thermally unstable (the time-scale for the instability is about 10^6 years), so the authors identify phase F as the intercloud medium. The authors pointed out that another stable phase should exist above 10^6 K, with brehmsstrahlung the chief cooling process.

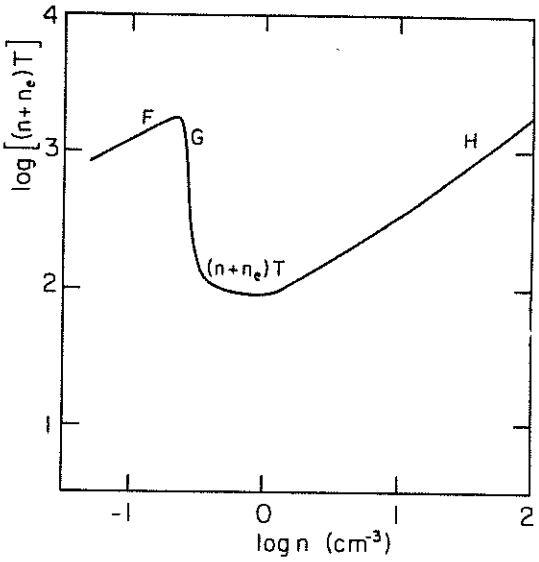

Fig. II.1.1 - Thermal pressure $P/k = (n+n_e)T$ versus gas density n, in the model of Field, Goldsmith and Habing (1969).

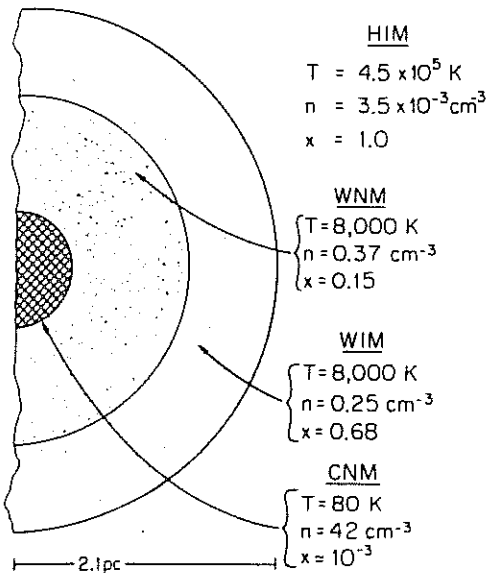

Fig. II.1.2 - Cross section of a characteristic small cloud, according to the model of McKee and Ostriker (1977). Typical values of hydrogen density, n, temperature, T, and ionization, $x=n_e/n$ are shown for each component: cold neutral medium (CNM), warm neutral medium (WNM), warm ionized medium (WIM), and hot ionized medium (HIM).

It is important to note that the phases thermally stable in the ISM are characterized by well defined ranges in temperature: $T < 100$ K, $T \sim 10^4$ K and $T \sim 10^6$ K. This fact can be explained in terms of the atomic properties of the gas, which control its radiative cooling (Appendix 1), and is not specific to the model for heating the gas. In fact, it is possible to produce models with different heating mechanisms, but with similar temperature distribution.

The 2-phase model of Field, Goldsmith and Habing has not been supported by UV absorption observations of HD and H_2, whose ratio implies a cosmic ray ionization rate in dense clouds that fail to meet the requirements of the model by more than one order of magnitude (Watson 1978).

The discovery of hot regions ($T \sim 10^5$ to 10^6 K) in the ISM by means of OVI absorptions lines and soft X-ray diffuse background (Sections I.1 and I.4), and the understanding of time-dependent mechanisms for heating the ISM (supernova explosions, stellar winds), naturally lead to the concept of a 3-phase ISM.

Cox and Smith (1974) found that a supernova outburst rate $\underline{r}$ on the order of 1 per 50 years in the disk of our Galaxy is sufficient to generate and mantain throughout the ISM a system of interconnected tunnels containing very low-density gas. The starting point of this model is that the hot low-density gas in the interior of a Supernova Remnant (SNR) radiates so inefficiently that the system will persist for a time $\tau > 4 \times 10^6$ years. The authors define a "porosity parameter" $q = r \tau V_{SNR}$, where V_{SNR} is the average final volume of the SNR. The fraction $\underline{f}$ of interstellar space occupied by the SNR's is $f \sim q$ for q

$<<$ 1. Cox and Smith estimate $q \sim 0.1$. However, once $q > 0.1$, there is a substantial chance for a given SNR to encounter another before it grows to its final volume. If that happens, the old SNR can be rejuvenated by the blast wave from the new one, which propagates preferentially in the low-density gas. In this way, a substantial fraction of the blast energy of supernovae can be released into an interconnecting tunnel system, which would occupy roughly half the interstellar volume.

McKee and Ostriker (1977) proposed a 3-phase model regulated by supernova explosions in an inhomogeneous substrate, combining the theory of SNR evolution (Appendix 3) and the theory of conductive interfaces (Spitzer 1962; Cowie and McKee 1977; McKee and Cowie 1977) within the framework of the Cox and Smith model. The resulting model consists of cool clouds embedded in a hot substrate which occupies a large fraction of the interstellar volume. A stationary cycle of mass flow is maintained in a balance between evaporation of the clouds and the addition of matter to the clouds from the hot gas by the sweeping action of supernova blast waves. By taking into account the radiative losses at the conductive interfaces between the clouds and the hot gas, McKee and Ostriker obtain analytical formulae for the mean pressure, density and temperature of clouds and hot gas and for the fractional volume occupied by each. According to this model, the clouds consist of a cold core ($T < 100$ K) surrounded succesively by a layer of warm ($T \sim 10^4$ K) HI, partially ionized and heated by soft X-rays and cosmic rays as in the model of Field, Goldsmith and Habing (1969), and then by a layer of warm ($T \sim 10^4$ K) HII. The outer layers of the clouds comprise a large fraction of the cloud volume but not of

the mass. In Fig. II.1.2 is shown a cross section of a typical cloud predicted by the model, together with typical values of the relevant physical parameters of the components.

By assuming a spectrum of cloud sizes, a mean interstellar density, a mean supernova rate and blast energy, the model of McKee and Ostriker accounts for the observed pressure of interstellar clouds (P/k = 2000-4000 K cm^{-3}), the galactic soft X-ray background, the OVI absorption line observations, the ionization and heating of much of the ISM, and even for the velocity dispersion ($\sim$ 8 km/s) of interstellar clouds. Probably the greatest weakness of the model concerns the warm material, which is predicted to be only 4% in the plane (including either ionized and neutral), while Spitzer (1978) gives 14% for the same fraction. An other weak point of the model is the morphology of the clouds, assumed to be spherical: modern observations and theories imply that the clouds are actually more like sheets, or even inhomogeneous filaments, which must have different surface-to-volume ratios from spheres.

Another theoretical approach for the physics of the ISM consists in taking into account the effects of stellar winds of early-type stars. In Appendix 3 we give a brief report of the interaction of such winds with the ISM. Of course, a global model for the ISM should consider both the effects of SNR's and those of stellar winds. An important characteristic of taking into account both effects is that the SNR's propagate through a medium which has been partially swept up by the action of the winds. The combined effect of SNR's and stellar winds leads to the production of large bubbles which consist of a hot interior (10^6-10^7 K) at low density (10^{-2}-10^{-4} cm^{-3}),

surrounded by a thin dense shell of temperature 10^2-10^4 K and density 1-100 cm^{-3}. The expanding shells are the main source of the kinetic energy of the ISM, e.g. of the bulk motions of the interstellar clouds. The hot bubbles are the main source for producing the hot component of the ISM.

Bruhweiler et al. (1980) computed the evolution of a large bubble produced by collective stellar winds within an OB association. They showed that the HI shells, detected by means of radio observations (Section I.2), are a natural product of the interaction of stellar winds and supernovae with the surrounding interstellar medium. Comparison of the predicted shell sizes and shapes as a function of their distance from the galactic center, with the predicted ones shows general agreement. This model also predicts that about 30% of the volume of the galactic plane will consist of superbubbles.

References

Bruhweiler,F.C., Gull,T.R., Kafatos,M., Sofia,S.: 1980, Astrophys. J., 238, L27.

Cox,D.P., Smith,B.W.: 1974, Astrophys. J., 189, L105.

Cowie,L.L., Songaila,A.: 1986, Ann. Rev. Astron. Astrophys., 24, 499.

Field,G.B., Goldsmith,D.W., Habing,H.J.: 1969, Astrophys. J., 155, L149.

McCray,R., Snow,T.: 1979, Ann. Rev. Astron. Astrophys., 17, 213.

McKee,C.F., Ostriker,J.P.: 1977, Astrophys. J., 218, 148.

Spitzer, L., Jr., 1978, Physical Processes in the Interstellar Medium, John Wiley and Sons, Inc..

Watson,W.D.: 1978, Ann. Rev. Astr. Astrophys., 16, 585.

2. THE HOT LOCAL INTERSTELLAR MEDIUM

Recent models have been developed in order to explain the observed soft X-ray background and its spectral shape, and also the measured OVI absorptions which arise from a gas slightly colder than that responsible for the soft X-ray emission. Usually, in these models the warm and the cold regions of the LISM are not taken into account, since the interaction between the hot phase and colder phases is very weak. The cold material has too high a space density and high a column density to be affected by the hot gas.

Innes and Hartquist (1984) used a simple model for the thermal properties of very old SNR's and superbubbles and proposed that the sun could be embedded in an old superbubble in radiative phase. In fact, they found that the observed soft X-ray background and extreme ultraviolet spectra can be produced by a superbubble formed by the injection of about 10^{52} erg into the LISM roughly 4×10^{6} years ago. The most interesting feature of this model resides in the spectrum hardening (as compared to the spectrum of adiabatic SNR), which results from the shape of the cooling curve versus temperature (see Appendix 1). Indeed the hotter gas takes much longer time to cool down than the originally cooler gas which lies closer to the edge of the bubble. Assuming the initial energy and the age indicated above, together with a density and pressure of the surrounding medium of 10^{-24} g cm^{-3} and 7×10^{4} K cm^{-3} respectively, the proportion of the hot

gas left in the interior at the present time is large enough to account for the B and C band fluxes, and even for the fluxes measured in softer (Be) and harder (M) bands. Since a lot of radiative losses occurred till the present epoch, the initial energy required to explain the present day thermal energy is very high, but not unreasonable: typically it amounts to the energy released by stellar winds and supernovae of an entire OB association. Besides, this model yields an OVI column density of $\sim 6 \times 10^{12}$ cm^{-2}, which is in agreement with the observed values in the LISM, i.e., N(OVI) $\lesssim 10^{13}$ cm^{-2}. Moreover, this OVI component will show a low velocity since the bubble is very old, thus a very good agreement with the OVI observations is achieved (Section I.1). Unfortunately this model requires a very high pressure ($\sim 7 \times 10^{4}$ K cm^{-3}), much too high to be reasonable in the light of the present day data. The pressure of the model could be lowered substantially if one does not require the reproduction of the EUV background, the origin of which could be attributed to cloud-hot gas interfaces (Stern and Bowyer 1979).

Cox and Anderson (1982) proposed a simple analytical approximation for the hydrodynamical evolution and structure of a SNR when the external medium pressure cannot be neglected with respect to the shock pressure. They computed the structure of the SNR for blast waves of initial energy $E_o = 5 \times 10^{50}$ erg in a hot, low-density interstellar environment. The ionization structure of the remnant was determined following the history of each shell from the time it was shocked up to the present time. They showed that the B and C bands of the soft X-ray background are reproduced by such a model if the ambient density is about 0.004 cm^{-3}, the blast radius is roughly

100 pc, and the sun is located inside the shocked region. The age of such an explosion is roughly 10^5 years.

The model of Cox and Anderson gets into severe trouble with the OVI observations: for blast waves propagating into homogeneous low-ionization material, the computed OVI column densities within the bubble exceed the observed values in the LISM by least a factor of 4. However, the OVI produced near the blast wave of a SNR with a shock temperature $T \sim 10^6$ K would be seen in absorption with a radial velocity of several hundreds km/s, while the observed profiles show a quasy null radial velocity, so Arnaud and Rothenflug (1986) think it is not meaningful to compare the observed OVI column densities with those computed in the framework of the Cox and Anderson model. A problem remains open: no component of OVI at high radial velocity has even been detected. It is possible that in hot gases, because of turbulence, the absorption lines of OVI are too broad and lost in the continuum, a possibility originally suggested by McKee and Ostriker (1977).

Thermal evaporation may occur as a consequence of heat conduction at the interface between a hot ($T > 10^6$ K) gas and colder clouds. Cowie (1984) pointed out the importance of taking into account this process in describing the hot gas in the local SNR. In fact, the evolution of a SNR remnant with thermal evaporation from embedded cold and warm material has radically different appearance from the classical non-evaporative models. The evaporative model succeed to explain the OVI column densities and radial velocities produced by the local gas (Cowie at al. 1980).

References

Arnaud,M., Rothenflug,R.: 1986, Proceedings of the XXVI COSPAR meeting, Toulouse, July 1986, Symposium no. 7, in press.

Cox,D.P., Anderson,P.R.: 1982, Astrophys. J., 253, 268.

Cowie,L.L.: 1984, IAU Coll. 81, "Local Interstellar Medium", NASA CP-2345, p. 287.

Cowie,L.L., Jenkins,E.B., Songaila,A., York,D.G.: 1980, Astrophys. J., 232, 467.

Innes,D.E., Hartquist,T.W.: 1984, M.N.R.A.S., 209, 7.

McKee,C.F., Ostriker,J.P.: 1977, Astrophys. J., 218, 148.

Stern,R., Bowyer,S.: 1979, Astrophys. J., 230, 755.

3. THE WARM LOCAL INTERSTELLAR MEDIUM

The material which can provide a mass source and energy sink to the hot gas is the warm (10^4 K) material which must form, given the presence of the cold gas. Given a typical UV flux, standard interstellar pressures and the presence of the cold gas, ionized warm material will rapidly occupy a significant fraction of the interstellar medium. Presumably, a substanctial fraction of neutral warm material forms too, for which we have no good heating mechanisms available.

The region around the sun appears to be occupied by material with density and temperature somewhat like those of the old "intercloud" medium of 2-phase ISM models. In this case, however, it is itself a very diffuse "cloud" in a much lower density environment, and seems to have a rather substantial ionization fraction. It is unclear how representative the local cloud is of the warm phases in the general ISM.

Frisch (1986) reviews the observations of interstellar gas in front of nearby ($d < 10$ pc) stars, to obtain the properties of the local warm cloud. She concludes that the temperature and the density are $T \sim 11500$ K and $n(HI) \sim 0.1$ cm^{-3} respectively. From MgI data she derives that the cloud is essentially neutral, with $n_e < 0.003$ cm^{-3}. The thermal pressure associated with this warm neutral cloud would be $P/k \sim 1200$ K cm^{-3}. This is a low value with respect to the mean value

found by Jura (1975) from an analysis of molecular hydrogen in 6 clouds not near HII regions ($P/k \sim 3600$ K cm^{-3}); to the value usually estimated from 21 cm observations ($P/k \sim 2000$ K cm^{-3}; Field 1975), and to the typical value derived by McKee and Ostriker (1977) from their general theory on the ISM ($P/k \sim 3700$ K cm^{-3}).

These results are not in agreement with backscattering measurements within the solar system (Section I.6), which give a temperature and neutral hydrogen density $T \sim 8000$ K and $n(HI) \sim 0.03$ to 0.06 cm^{-3}, together with a helium density $n(HeI) \sim 0.015$ to 0.020 cm^{-3}. Assuming that helium is not ionized and a cosmic ratio [H/He] = 10, these measurements imply a significant degree of ionization: $n_e / n(H) \sim 0.60$ to 0.85 with $n(H) = 0.15$ to 0.20 cm^{-3}. According to these data the local cloud is composed of warm ionized material, similar to the one present in the outer shell of the clouds in the McKee and Ostriker model (see Fig. II.1.2). Moreover, the cloud has physical properties very similar to the wide-spread warm phase of the ISM associated with the pulsar dispersion measures and the interstellar emission-line background (Section I.2). The total thermal pressure of the cloud, taking into account n(HII) and n_e, is $P/k \sim 2600$ K cm^{-3}, i.e., more similar to the above reported observational and theoretical values. It is important to note that the directly observed neutral atoms provide a thermal pressure of only $P/k \sim 500$ K cm^{-3}, which is another argument in favour for the presence of a significant degree of ionization.

Reynolds (1986) points out that the ionization rate per hydrogen atom derived using backscattering results is much larger than that due to cosmic rays or the soft X-ray background. An examination of

available data on B stars and known white dwarfs in the solar neighborhood reveals that the photon flux from these sources also is not capable of accounting for such a high ionization rate. One way to explain this discrepancy is to assume a transient event within the last $2\text{-}5\times10^5$ years. In fact, in a gas of $T \sim 10^4$ K with a density of 0.2 cm^{-3} the cooling time scale is about 2×10^5 years (Kafatos 1973), while the corresponding recombination time scale is 5×10^5 years. Thus the inferred temperature and ionization fraction of the gas imply that the ionization and heating occurred less than $2\text{-}5\times10^5$ years ago. Cox and Anderson (1982) have shown that a supernova approximately 10^5 years ago within 100 pc of the sun would explain many characteristics of the diffuse X-ray background (Section II.2). Although the low velocity of the local gas (16 km/s with respect to the LSR) suggests that it has not interacted recently with a strong shock, an intense flux of ionizing radiation from the supernova or its remnant could have affected the gas.

Another potential source of ionization proposed by Reynolds (1986) in order to explain the local hydrogen ionization rate is a diffuse flux of EUV radiation possibly associated with a nearby region of $\sim 10^5$ K. This is consistent with available flux measurements (or upper limits) obtained from far UV to soft X-ray.

Of the known sources of ionization, it appears that only O stars produce a flux that is sufficient to account for the ionization of the diffuse warm gas responsible of the H_α emission background (Mathis 1986). The apparent absence of a stellar contribution to the ionization of the very local gas suggests that luminous stars are not the sole source of ionization for the diffuse ISM.

We conclude pointing out that the pressure of the local warm cloud is significantly lower than that derived from the analysis of the soft X-ray background ($P/k \sim 10^4$ K cm^{-3}). Due to this fact, this cloud may be in the process of being imploded and ablated by the high pressure of the hot gas. A thermal evaporation mechanism may act at the edge of the diffuse cloud towards the hot 10^6 K tenuous surrounding medium.

References

Field,G.B.: 1975, in Physique et Moleculaire et Materie Interstellaire (Les Houches 1974), ed. R.Balian et al., (Amsterdam:North-Holland).

Frisch,P.C.: 1986, Proceedings of the XXVI COSPAR meeting, Symposium no. 7, Toulouse, July 1986, in press.

Kafatos,M.: 1973, Astrophys. J., 182, 433.

Jura,M.: 1975, Astrophys. J., 197, 581.

Mathis,J.S.: 1986, Astrophys. J., 301, 423.

Reynolds,R.J.: 1986, Astron. J., 92, 653.

4. THE COLD LOCAL INTERSTELLAR MEDIUM

The cold neutral gas has a high density and is clumped into structures with a relatively high column density, so its global evolution is not strongly affected by the presence of the hot phase of the ISM. For this reason, the models of the hot LISM (Section II.2) do not take into account the observed structures of the cold nearby interstellar gas, but only the observations strictly related to the hot gas (soft X-ray background, OVI absorptions). However, the observations of the cold gas give unique informations on the global structure and dynamics of the LISM, while the observations of the hot gas (OVI and soft X background) are mainly concerned with its physical state (temperature structure, ionization structure ...). So, the two are complementary, and future efforts should be devoted to build global models which take into account both aspects of the problem. Future models must also take into account the small nearby molecular clouds detected by means of millimetric and infrared observations (Section I.5). Here we briefly review two evolutionary models of nearby large-scale structures of neutral hydrogen revealed by means of 21 cm observations.

Weaver (1979) after summarizing and discussing the data available for the region of the sky around $\ell = 330^{\circ}$ (Section I.3), proposed a model which combines the effects of stellar winds and the explosion of a supernova (Appendix 3) from the Sco-Cen association. Between 1 and

2×10^7 years ago the Sco-Cen group formed. A considerable amount of interstellar material remained after the first period of star formation. The strong stellar winds from the massive stars inflated a bubble of gas and dust, concentric with the Sco-Cen association, sweeping up the unused interstellar material. As the denser clumps were swept up on the expanding bubble, they were compressed in the radial direction, stretched into the HI filaments we see today. In this model, Loop I is a SN shell produced by the explosion of one of the most massive members of Sco-Cen. The explosion occurred inside the bubble, so the shell expanded in a tenuous uniform medium mantaining a closely spherical form and reaching a large size. This shell is just beginning to interact with and further accelerate the gas at the surface of the bubble. Preliminary calculations indicate that the expanding bubble contains 10^6 $M_\odot$ of gas, has a total kinetic energy of is $\sim 10^{50}$ erg , and a diameter of $\sim$ 300 pc.

It is important to note that the Sco-Cen association is centered at $\ell = 330^\circ$, $b = +15^\circ$, i.e., a direction angularly close to the origin of the LISM motion derived by Crutcher (1982; Section I.1) from his analysis of optical absorption lines of TiII. So, Weaver's model offers a natural explanation for the kinematics of the nearby neutral gas. Taking into account that the nearest side of the expanding shell should be within a few tens of parsecs of the sun (radio observations; Section I.3), that the distance to Sco-Cen is $\sim$ 170 pc, and that the LSR velocity of the gas from Sco-Cen has a module of 15 km/s (Crutcher's analysis), we obtain an expansion age of $\sim 10^7$ years, which is consistent with the nuclear age of the stars in the association. We conclude that Weaver's model seems to be able to

explain radio and optical observations of nearby cold gas. Moreover, according to Berkhujsen (1973), the age of Loop I is ~ 10^6 years: this is consistent with Weaver's suggestion, according to which the supernova exploded after the creation of the bubble by means of the stellar winds.

Let us now discuss some models, related to the HI 21 cm observations of ring of gas associated to the Gould belt (*). Since the sun lies well inside the Gould belt structure, understanding the origin and evolution of this system of cold gas and stars should help one to put constraints on evolutionary models of the LISM.

(*) The O and B stars near the sun define roughly two great circles on the sky: one aligned along the Milky Way, and the other, studied by Gould (1879) and called the Gould belt, inclined to it by about 20°. Radio observations of the 21 cm emission of HI have also revealed the presence of a ring of cold gas associated to distribution of stars in the belt (Lindblad 1967). Stothers and Frogel (1974) demonstrated statistically the reality of the Gould belt as an independent system in the local region of our galaxy, connected with the existence of an eccentric "hole" of ~ 200 pc diameter in the distribution of OB stars and interstellar dust around the sun. They found that the Gould belt is about three times compressed vertically than is the galactic belt, and has an inclination of about 18° to the IAU plane, with the direction of the tilt towards Orion. It extends as much as ~ 800 pc in that direction and ~ 300 pc towards Ophiucus. The sun lies effectively in the mean plane. A crude "diameter" of the system is 750-1000 pc, with the formal center of the star positions lying 150-250 pc towards Orion. The longitude and latitude of the North Pole of the Gould belt in galactic coordinates are $\ell = 205 \pm 1$ and $b = +72 \pm 1$ respectively. Frogel and Stothers (1977) studied the kinematics of the local complex of O and B stars and found that the youngest stars of the belt represent a local perturbation of the general galactic differential rotation. If we interpret this fact as due to linear expansion of the Gould belt as a whole at ~ 4 km/s, such a velocity implies an <u>expansion time</u> of 7×10^7 years.

As was pointed out by Lindblad (1967), the observed velocity -longitude relation of the gas ring is characteristic of material expanding in a field of differential rotation. Lindblad et al. (1973) used a model in which the interaction between the ring and the interstellar matter was assumed negligible to fit the observed velocity-longitude relation.

Olano (1982) proposed a model of the Gould belt as an expanding ring of gas, including the effects of the braking force due to the interaction between the expanding gas and the surrounding interstellar gas. In this model it is assumed that the outer part of ring is moving with constant momentum and is sweeping up galactic gas ("snowplough model"; see Appendix 3). By fitting the model to the radial velocities from the 21 cm observations, it is found that the center of the ring is in the direction $\ell \sim 131^{\circ}$, at a distance from the sun of 166 pc. An age of 3×10^{7} years and a mass of 1.2×10^{6} $M_{\odot}$ is obtained for the system. The ring would have been originated by the interaction of stellar winds and supernovae, originated in the Cas-Tau group, with the surrounding ISM. The determined age implies that only the younger stars of the expanding local group of stars would have been formed in the ring or by its influence. In particular, the Sco-Cen association, and other slightly younger associations (I Ori, II Per, I Lac), might be related to the gas of the belt. We don't exclude the possibility that the expanding ring of gas triggered the processes of star formation in these associations. In this case, Weaver's model for the interaction of the Sco-Cen group with the surrounding ISM should be linked to the evolutionary models of the Gould belt as a whole.

References

Berkhuijsen,E.M.: 1973, Astron. Astrophys., 24, 123.

Crutcher,R.M., 1982, Astrophys. J., 254, 82.

Frogel,J.A., Stothers,R.: 1977, Astron. J., 82, 890.

Gould,B.A.: 1879, Uranometria Argentina (P.E. Coni, Buenos Aires), p. 355.

Lindblad,P.O.: 1967, Bull. Astron. Inst. Neth., 19, 34.

Lindblad,P.O., Grape,K., Sandqvist,Aa., Schober,J.: 1973, Astron. Astrophys., 24, 309.

Olano,C.A.: 1982, Astron. Astrophys., 112, 195.

Stothers,R., Frogel,J.A.: 1974, Astron. J., 79, 456.

Weaver,H.: 1979, in The Large Scale Characteristics of the Galaxy, IAU Symp. 84, ed. W.B.Burton (Dordrecht:Reidel), p. 295.

THIRD PART

STUDY OF THE LISM TOWARDS NEARBY COOL STARS

1. INTRODUCTION

The MgII h and k resonance transitions are among the most sensitive lines suitable for exploring the ISM in the solar neighbourhood. In fact, magnesium is one of the most abundant elements (log [H/Mg] = 4.46; Withbroe 1971); it exists mainly in the singly ionized state in those parts of the ISM where atomic hydrogen is neutral (Bruhweiler et al. 1984) and the lines of its resonance doublet have high oscillator strengths (f = 0.627 and 0.313; Wiese et al. 1969).

The MgII interstellar absorptions have been studied towards the few early type stars (Kondo et al. 1978) and hot white dwarfs (Bruhweiler and Kondo 1982) situated in the solar environment. It is clear that the small number of early-type stars available in the solar neighbourhood make it impossible to use them for sampling many lines of sight within a few tens of parsecs. Late-type stars are much more numerous in the local region and can provide a suitable background spectrum for observing the interstellar MgII absorptions.

In the late-type stars the temperature rise above the photosphere acts on the collision-dominated source function of the MgII h and k transitions in such a way to produce an emission line whose detailed profile depends on the physical state and velocity fields as a function of the optical depth in the chromosphere. Usually a central absorption is present at the top of the chromospheric MgII emissions,

also originated in the stellar chromosphere. Some years ago Bohm-Vitense (1981) advanced the idea of an interstellar contribution to the central absorption observed in the MgII emissions of cool stars, noting a correlation between the position of the central absorption and the star's radial velocity.

More recently, we have obtained high resolution IUE spectra containing the MgII resonance doublet for a group of especially selected cool dwarfs and giants. We have shown that interstellar MgII absorptions can be detected in the chromospheric emissions of cool stars, provided the interstellar feature is displaced from the top of the emission profile (Vladilo et al. 1985). In this case it is possible to distinguish a truly chromospheric central absorption (self-reversal) from the interstellar line which falls on the wings of the emission profile. An example of this is shown in Fig. III.1.1, where we plot the region of the MgII k line in a IUE spectrum of βHyi. We see that within the emission line are two distinct absorption features, one at +8 km/s and the other at -23 km/s with respect to the photospheric rest frame. It is reasonable to assume that the +8 km/s feature is chromospheric, but the -23 km/s feature must be either circumstellar or interstellar. There are two reasons to reject the circumstellar hypothesis. The first is that the radial velocity of the component is equal and opposite to that of the star (RV = +23 km/s); this would imply a circumstellar shell expanding at exactly that velocity: an improbable coincidence. Secondly, β Hyi falls well below the line first indicated by Reimers (1977) on the H-R diagram which differentiates stars showing significant mass outflow from those which do not.

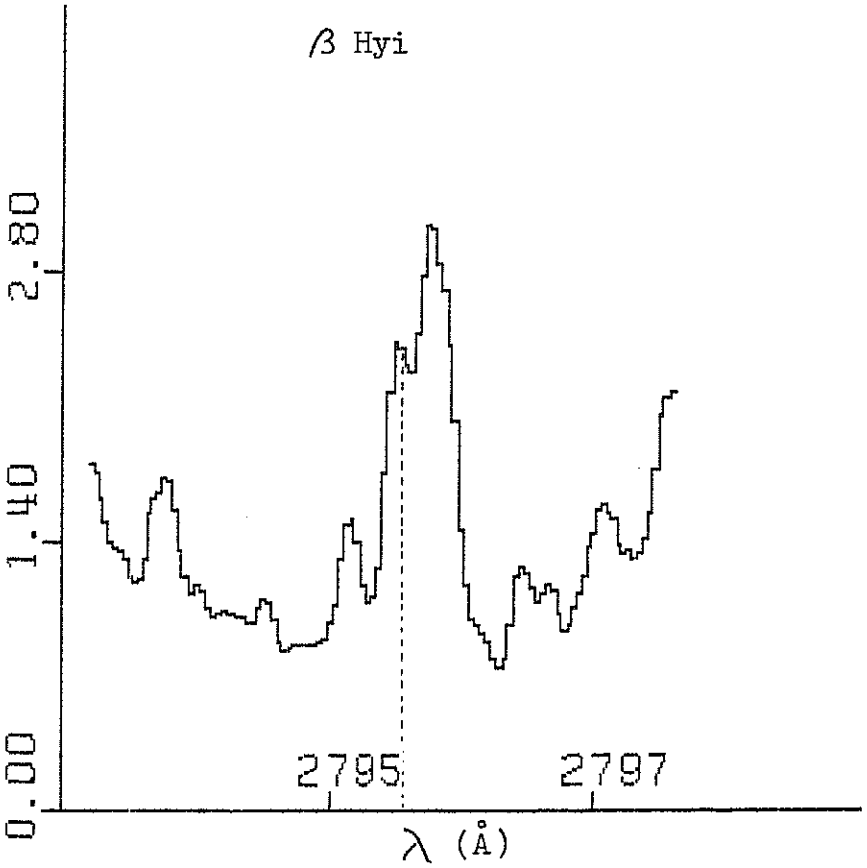

Fig. III.1.1 - MgII k line in β Hyi with superimposed the rest wavelength with respect to the photospheric frame (dashed line).

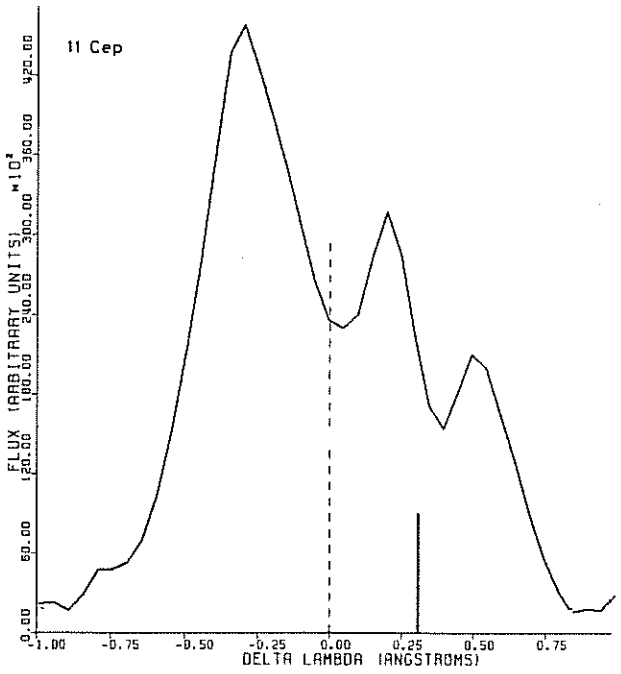

Fig. III.1.2 - MgII k line in 11 Cep with superimposed the rest wavelength with respect to the photospheric frame. The vertical bar indicates the predicted position of the interstellar absorption.

We have also detected MgII absorptions red-shifted with respect to the stellar rest frame in a sample of specially selected nearby cool giants (Molaro et al. 1986). Since red-shifted absorptions are not believed to be originated in circumstellar shells, this is a strong argument in favour of the interstellar nature of the detected features. One example is shown in Fig. III.1.2, where one can see the interstellar absorption clearly separated from the chromospheric self-reversal.

A major result of these observations has been that, in order to explain the position of the observed features, an interstellar wind such as that proposed by Crutcher (1982) towards more distant stars (Section I.1) must also be present at short distances (e.g. towards β Hyi which is at 6.3 pc). The detection of features both blue-shifted and red-shifted, and exactly at the position predicted by Crutcher's model, confirms the interstellar nature of the observed absorptions and allows us to use this model to investigate new lines of sight.

Only stars with particular radial velocities along a given line of sight can be used to observe the interstellar absorption well separated from the self-reversal. In the majority of cool stars, the interstellar MgII absorptions are not distinguishable from the self-reversals at the IUE resolution (FWHM $\sim$ 20 km/s), instead they produce stronger central absorptions or asymmetries in the stellar emissions. In the present work we analyze the IUE spectra of 91 cool stars in a systematic search for interstellar absorptions in MgII emission profiles. The main purpose of this work is to study the kinematics, the distribution and the physical state of the local gas in a very

large number of lines of sight, establishing limits to the interstellar magnesium column densities even when the absorption is blended with the chromospheric self-reversal.

We have collected 150 IUE high resolution spectra of cool stars taken from the VILSPA data bank, of spectral types ranging from F5 to K5 and luminosity classes between V and III. Spectroscopic binaries have been excluded. After rejecting the stars for which only noisy spectra were available from the data bank, we have retained a sample of 91 stars whose relevant data are given in Table III.1. In the first three columns of the Table we give a running number, the HD number, and the distance, d (pc). The stars selected are located within 100 pc of the sun, 62 of them being within 25 pc. Trigonometric parallaxes have been used for stars closer than 25 pc and spectroscopic parallaxes for stars at greater distances. Typical errors introduced by the distance uncertainties are of the order of 30% (spectroscopic distances) or lower (trigonometric distances).

In the fourth, fifth and sixth columns we give the galactic coordinates, ℓ and b (°), and the star's radial velocity, RV (km/s). In the last column of Table III.1 we give the predicted heliocentric velocity of the interstellar gas along the line of sight, Vis (km/s) derived using the following relation (Crutcher 1982):

$$Vis = V_o \left[\sin b \sin b_o + \cos b \cos b_o \cos(\ell - \ell_o)\right] , \qquad (1.1)$$

with

$V_o = -28$ km/s, $\ell_o = 25°$, $b_o = +10°$.

The heliocentric velocity of the interstellar gas, Vis, can be transformed to the photospheric frame of the star, using the relation:

$$\Delta Vis = Vis - RV \ . \qquad (1.2)$$

The wavelength scale of the IUE spectra has been reduced to the photospheric frame, using a set of 9 photospheric lines near the MgII doublet (Franco et al. 1984). This calibration allows us to compare the radial velocities of the observed interstellar absorptions with the predicted values, ΔVis. The typical error resulting from the wavelength calibration procedure is $\Delta\lambda \sim 0.04$ Å, corresponding to an uncertainty in the velocity $\Delta v \sim 4$ Km/s.

Table III.1

	HD	d	l	b	RV	Vis
1	166	15	111	-33	-8	1
2	1522	52	99	-70	19	2
3	1835	20	97	-74	-7	2
4	2151	6	305	-40	23	-1
5	4128	16	111	-81	13	5
6	5395	20	124	-4	-47	5
7	9562	36	151	-68	-15	11
8	9927	58	131	-14	16	9
9	10307	12	133	-19	4	10
10	10700	3	173	-73	-16	11
11	12929	23	145	-36	-14	14
12	16895	12	141	-10	25	13
13	17925	8	192	-58	19	18
14	19994	18	182	-47	18	21
15	23249	9	198	-46	-6	23
16	23817	20	279	-44	51	9
17	25680	16	171	-22	26	23
18	25998	20	160	-10	25	20
19	27442	15	270	-43	29	12
20	28305	46	178	-20	39	25
21	29139	20	181	-20	54	25
22	30495	13	215	-35	23	25
23	33262	12	266	-37	-2	14
24	36079	97	224	-27	-14	25
25	38393	8	227	-24	-10	25
26	39587	10	188	-3	-14	27
27	43039	65	183	6	20	25
28	47205	17	229	-12	3	26
29	52711	17	187	15	22	24
30	63295	56	285	-22	48	6

	HD	d	l	b	RV	Vis
31	68456	18	275	-15	25	10
32	71369	41	156	35	20	12
33	72905	14	15	36	-12	10
34	76294	29	22	30	23	20
35	81797	44	242	29	-4	17
36	82210	24	143	39	-27	7
37	82885	9	188	48	13	14
38	84117	13	257	22	34	14
39	84737	14	173	49	5	12
40	85444	58	251	29	-15	14
41	91324	20	283	4	20	5
42	94264	42	190	64	16	7
43	95272	32	269	37	47	7
44	99984	34	163	67	-30	4
45	101501	8	184	73	-5	3
46	102870	10	270	61	5	1
47	104979	26	270	69	-30	0
48	105707	43	291	39	5	-2
49	108570	48	300	6	8	-3
50	109379	29	298	39	-8	-4
51	111456	24	124	57	-12	-2
52	114710	8	43	85	6	-7
53	115383	13	323	71	-26	-9
54	117176	23	338	74	5	-10
55	120136	17	359	74	-16	-12
56	123139	15	319	24	1	-12
57	126660	14	94	60	-11	-9
58	131156	6	23	61	3	-18
59	131873	26	113	41	17	-4
60	137759	25	94	49	-11	-10

	HD	d	l	b	RV	Vis
61	140573	19	14	44	3	-23
62	141714	71	42	50	-19	-21
63	142373	16	68	50	-55	-17
64	143761	25	54	49	18	-19
65	149661	11	14	28	-15	-26
66	150798	32	322	-15	-3	-11
67	150997	29	62	41	8	-20
68	151680	19	349	7	-3	-23
69	154417	22	21	24	-18	-27
70	161096	30	29	17	-12	-28
71	161797	8	52	26	-16	-24
72	163993	48	55	24	-2	-24
73	168723	17	27	5	9	-28
74	185144	6	101	22	27	-8
75	190248	6	330	-32	-22	-11
76	190406	17	57	-8	4	-22
77	191026	31	73	2	-33	-19
78	194012	29	57	-13	2	-22
79	196378	21	336	-37	-32	-12
80	197989	22	76	-6	-10	-17
81	199951	29	12	-40	18	-17
82	203387	30	34	-41	12	-17
83	203608	9	328	-40	-30	-8
84	206860	15	70	-28	-19	-15
85	209100	3	336	-48	-40	-8
86	215648	19	81	-40	-5	-9
87	216131	25	91	-31	14	-7
88	216228	24	111	6	-12	-2
89	217014	14	90	-35	-31	-7
90	220657	28	99	-35	-11	-3
91	222404	15	119	15	-42	1

2. KINEMATICS OF THE LISM

As we have seen in the prece ding Section, the radial velocities of the interstellar lines detected in our IUE spectra of especially selected nearby cool stars (Beckman et al. 1984, Vladilo et al. 1985, Molaro et al. 1986) are in agreement with the kinematics of the LISM derived by Crutcher (1982) using optical absorption lines towards stars within 100 pc (Section I.1). Here we have searched for interstellar features at the radial velocity predicted by Crutcher's model in the spectra collected from the IUE data bank.

The results of this analysis can be summarized as follows. The spectra of 40 stars of our sample (44% of the total) show clear interstellar absorptions, or at least asymmetries of the emission profiles, that can be explained as due to an unresolved interstellar feature at the predicted position, Vis. In 10 stars the predicted positions of the interstellar features fall outside the chromospheric emissions, so it is possible that we cannot detect them just because they fall in a spectral region with very low signal. In the remaining stars the interstellar absorptions are not observed, or are possibly blended with the chromospheric self-absorption, preventing us from reaching any conclusion about the velocity of possible interstellar components (nevertheless, many of these targets have been used in deriving upper limits to the MgII column density, as it is explained in the next Section). In none of the cases is there an absorption at

a position significantly different from the model prediction. All the data confirm the general presence of the interstellar absorption superposed on the chromospheric profiles.

In Fig. III.2.1 is shown the distribution of our targets on the sky in galactic coordinates. The filled symbols indicate the stars whose spectra show a clear absorption line, or at least a clear asymmetry of the emission profile, that can be explained by the presence of an interstellar component at the predicted position, Vis. The lack of interstellar features in the galactic longitude range $\ell = 120^\circ$ to $\ell = 240^\circ$ is interpreted as intrinsic low density of the gas (see next Section).

As we have seen in Section I.6, the analysis of interplanetary Lyα and HeI 584 backscattering (Bertaux 1984) confirms that the local gas is streaming through the solar system with a velocity of about 16 km/s (LSR), almost equal to that found by Crutcher (1982) for the interstellar nearby gas. Nevertheless, the directions of the velocity vectors derived with the two methods significantly disagree: Crutcher's wind flows from $\ell = 345^\circ$, $b = -10^\circ$, while Bertaux's wind from $\ell = 304^\circ$, $b = -4^\circ$ (LSR).

The origin of such discrepancy is at the moment unknown. If it were due to some local effect related to the interaction solar system/interstellar wind, the radial velocities of the interstellar absorptions towards nearby stars should obey the Crutcher's flow, even for the shortest lines of sight. Landsman et al. (1986) find that the projected interstellar wind velocity towards α Cen is in good agreement with Bertaux's flow, but this velocity determination, based

Figure III.2.1

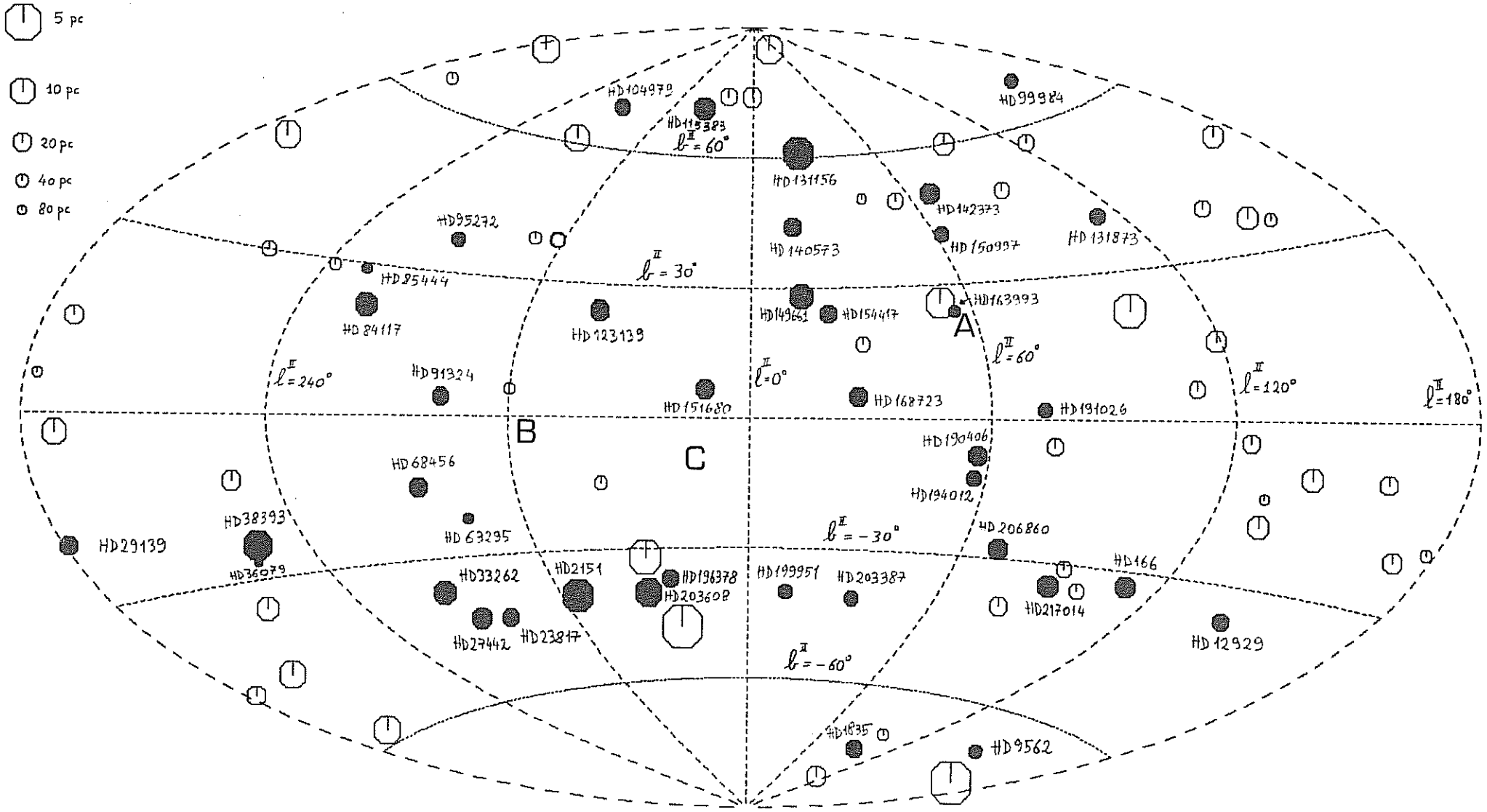

on fits of the broad interstellar Lyα absorption, may not be valid if the line of sight contains more than one interstellar component. Vidal-Madjar and co-workers identify (at least) two components in the lines of sight towards λ Sco and α Aql: the stronger has a radial velocity in agreement with Crutcher's velocity; the weaker with Bertaux's velocity (Ferlet et al. 1986, Vidal-Madjar et al. 1986a). According to these kind of observations the discrepancy is real, and the authors conclude that it is due to the existence of at least two local clouds streaming with different velocities.

The present investigation show that in a large number of lines of sight spread all over the sky, and with different distances to the target stars, the radial velocities of the observed MgII absorptions favour the direction found by Crutcher. Nevertheless, we do not exclude the possibility that the absorptions we see are blends of several components with different strengths and velocities, the stronger component obeying Crutcher's flow. The IUE resolution and signal-to-noise are in fact inadequate for solving weak components with separations of a few km/s such as those detected by Vidal-Madjar and co-workers.

Discussion

Small-scale kinematics - As we have seen in Section II.3, there is a pressure gradient between the hot regions revealed by the soft X-ray background ($P/k \sim 10^4$ K cm^{-3}) and the local warm cloud ($P/k \lesssim 2600$ K cm^{-3}). As a consequence, a velocity field oriented from the high-pressure hot gas, towards the low-pressure warm gas should be present

at the edge of the local cloud. Since the sun is situated near the edge of the warm diffuse cloud, one would expect to detect some local deviations from the general velocity field of the LISM derived by Crutcher and confirmed by the present work.

Let us make the working hypothesis that both the interplanetary neutral gas streaming at a LSR velocity $\underline{V}(B)$, as reported by Bertaux, and the weak component of the local interstellar gas streaming at a velocity consistent with $\underline{V}(B)$, detected by Vidal-Madjar, indicate the presence of a local velocity field, which is the result of the vectorial sum

$$\underline{V}(B) = \underline{V}(C) + \underline{V}(P) \ , \qquad (2.1)$$

where $\underline{V}(C)$ is the general velocity of the LISM clouds, as derived by Crutcher, and $\underline{V}(P)$ is the velocity of the gas moving from the edge of our cloud to its interior as a consequence of the pressure gradient. Of course, this hypothesis is attractive, since it would be able to explain the discrepancy between the gas velocity measured towards nearby stars, $\underline{V}(C)$, and that derived by means of backscattering observations, $\underline{V}(B)$. If the hypothesis is correct, $\underline{V}(P)$ should be oriented from the hot low-density region, towards the denser parts of the local environment. In order to perform this simple check of consistency, we have computed $\underline{V}(P)$ using relation (2.1), given the observational values of $\underline{V}(B)$ and $\underline{V}(C)$. The result is encouraging: $\underline{V}(P)$ lies as a first approximation in the galactic plane and is oriented from $\ell \cong 240^{\circ}$ towards $\ell \cong 60^{\circ}$, i.e., exactly from the middle of the "hole" of hot gas, towards the nearby strong density gradient visible in the global picture of Paresce (1984). The situation is

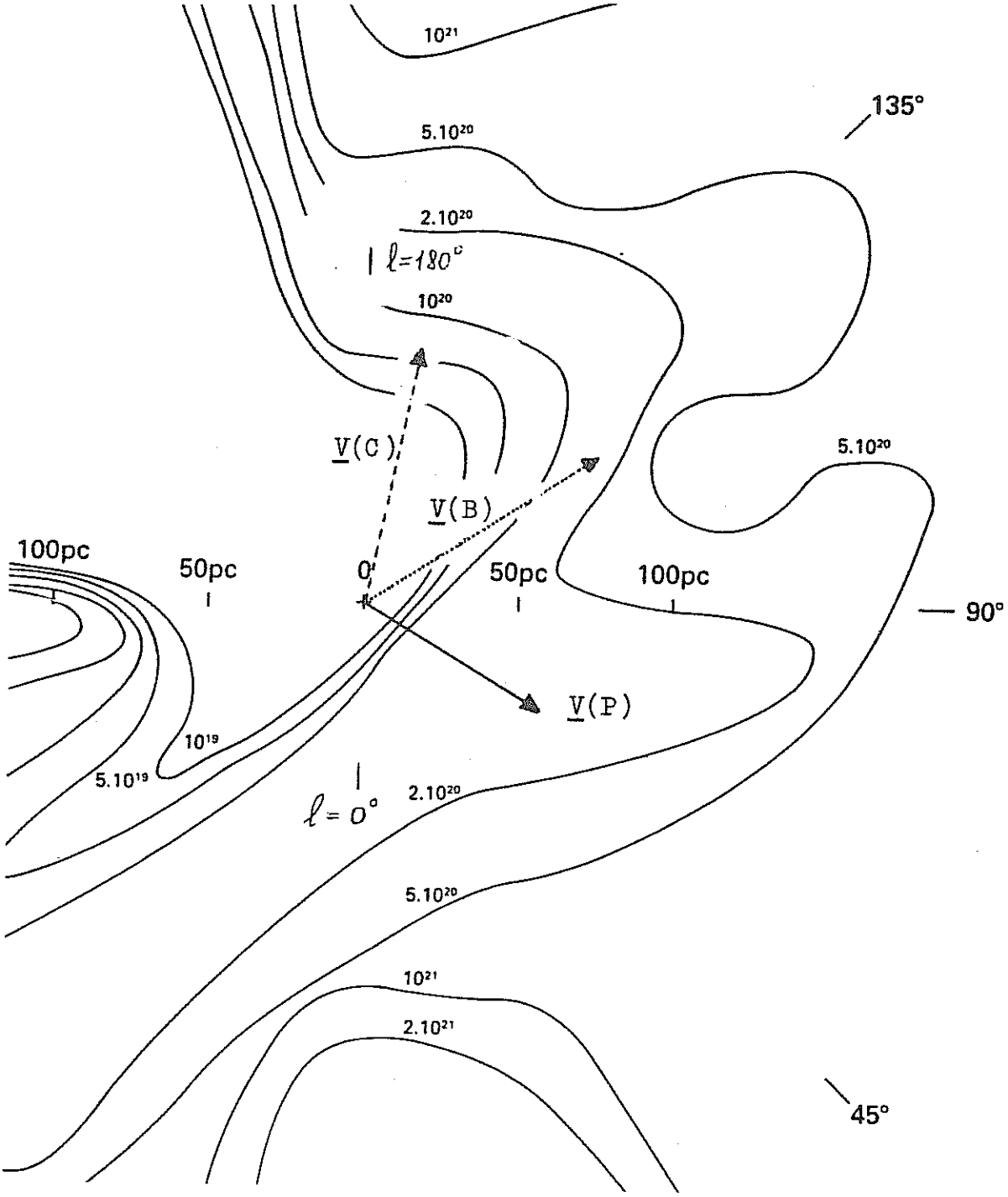

Fig. III.2.2 - Projection onto the galactic plane of the velocity vectors $\underline{V}(C)$, $\underline{V}(B)$ and $\underline{V}(P)$ defined in eq. (2.1). For comparison, we trace the contours of equal hydrogen column density taken from Paresce (1984).

illustrated in Fig. III.2.2, in which the result appears quite attractive, since the vector $\underline{V}(P)$ seems to sweep up the cold material and to compress the contours of iso-column density given by Paresce. $\underline{V}(P)$ has a module of 11 km/s, which would correspond to a slightly supersonic motion in a warm ($T \sim 10^4$ K) ionized material (sound velocity ~ 10 km/s; Spitzer 1978), and to a subsonic motion in the hot ($T \sim 10^6$ K) interstellar medium (sound velocity ~ 80 km/s; McKee and Ostriker 1977).

Of course, more refined observational tests and a detailed physical model should be taken into account for proving our hypothesis. A complete physical model should take into account the physics of conductive interfaces, the presence of magnetic fields, the turbulence created as a consequence of possible Rayleigh-Taylor instabilities at the border between the high-pressure tenuous ($n \sim 0.005$ cm^{-3}) gas and the low-pressure denser ($n \sim 0.1$ cm^{-3}) local cloud, and so on. This is out of the purposes of the present work.

Large-scale kinematics. - As we have seen in Section II.4, Weaver (1979) proposed a model for explaining the observational data available for the region of the sky centered around $\ell = 330°$. Crutcher (1982) suggested that Weaver's model offers a natural explanation for the LISM motion: the LISM is material which has been accelerated towards the sun from the direction of the Sco-Cen association. It represents the leading edge of an expanding shell. If we are near the edge of this expanding material, it would be interesting to study the downwind emisphere at large distances, in order to investigate the extension of the moving material. Among our targets, the best

candidate for this search is surely the star HD36079 (ℓ=224°, b=-27°), which is situated in the middle of the hole of the local neutral gas distribution, more than 120° away from the origin of the LISM motion, and at a distance of 97 pc. From the analysis of its IUE spectrum one can see a strong depression in the red peaks of the h and k chromospheric emissions, close to the predicted velocity Vis. A rough estimate of the magnesium column density gives log N(MgII) $\gtrsim$ 13.5. We compare this result with that found for the star HD38393 (ℓ=227°, b=-24°), which is angularly very close to HD36079, but only at 8 pc from the sun: for this line of sight we find log N(MgII) $\sim$ 12.5. These data imply that there is a considerable amount of material beyond HD38393, i.e., in the downwind emisphere, sharing the general velocity of the LISM. This result, in the frame of Weaver's model, would imply that the edge of the expanding material has already reached the downwind emisphere of the sky, and it is not situated in front of the Sco-Cen direction.

3. DISTRIBUTION AND PHYSICAL STATE OF THE LISM

Once we have shown that the interstellar absorptions, when present, fall at a radial velocity predicted by Crutcher's model, any absence of detectable features at the predicted position can be interpreted as the absence of a significant absorption by MgII ions along the line of sight. The fact that, as a first approximation, the stars at shorter distances do not show strong interstellar absorptions, while the more distant stars do, gives weight to this interpretation.

It is difficult and sometimes impossible to measure the equivalent widths, W(h) and W(k), of the h and k MgII absorptions, owing to the poor signal-to-noise ratio of the IUE spectra in the MgII region, and specially in the spectra collected from the data bank, whose exposure times may have been optimized for studying different spectral regions. Moreover, the saturation of the strongest absorption lines make it difficult the conversion from equivalent widths to MgII column densities, N(MgII). For the cases in which no interstellar features are present at the predicted position (an example is shown in Fig. III.3.1), we have assumed 40mA as the minimum equivalent width detectable in our spectra, in order to derive a conservative upper limit for N(MgII) using the linear part of the curve of growth. When present, the interstellar absorptions are generally saturated and only lower limits for N(MgII) can be derived

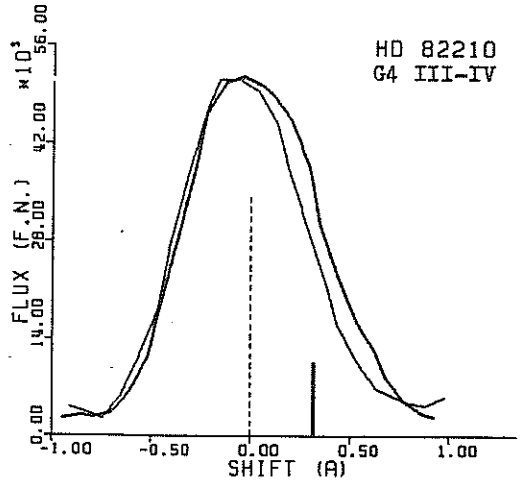

Fig. III.3.1 - MgII chromospheric emissions showing no trace of interstellar contamination. The h (thin line) and k (thick line) profiles have been superposed after subtracting from the photospheric wavelength scale the corresponding laboratory wavelengths. The thick bar indicates the predicted position, ΔVis, of the interstellar component, the dashed line the position of the rest wavelength in the photospheric frame.

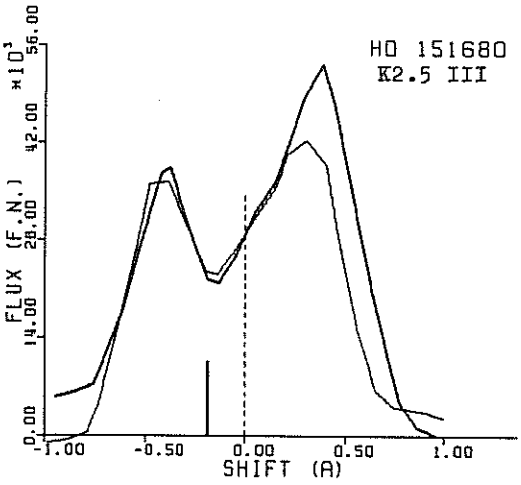

Fig. III.3.2 - MgII chromospheric emissions showing strong, saturated interstellar absorptions.

(see, e.g., Fig. III.3.2). When the absorptions are clearly saturated [i.e., W(k) ~ W(h)] and W(k) > 100 mA, we have assumed that the ratio W(k)/W(h) < 1.2 in order to derive a lower limit for N(MgII) by means of the doublet ratio method (Spitzer 1968). The stars for which we could derive lower or upper limits are reported in Table III.3.1.

TABLE III.3.1

HD	W(k) [mA]	log N(MgII) [cm^{-2}]	n(MgII) [10^{-7} cm^{-3}]
2151	150	>13.2	>7.8
10700	<40	<12.0	<0.84
12929	>115	>13.1	>1.7
17925	<40	<12.0	<0.36
25680	<40	<12.0	<0.18
25998	<50	<12.1	<0.19
29139	215	>13.3	>3.5
30495	<40	<12.0	<0.23
33262	>110	>13.1	>3.0
39587	<50	<12.1	<0.37
52711	<40	<12.0	<0.17
68456	230	>13.4	>4.2
71369	242	>13.4	>1.9
72905	<40	<12.0	<0.21
82210	<40	<12.0	<0.12
82885	<46	<12.1	<0.38
84117	171	>13.2	>4.3
101501	<40	<12.0	<0.35
104979	172	>13.2	>2.2
111456	<40	<12.0	<0.12
114710	<40	<12.0	<0.36
115383	<40 W(h)	<12.3	<0.45
120136	<50	<12.1	<0.22
126660	<50	<12.1	<0.27
131156	<40	<12.0	<0.46
131873	450	>13.7	>5.7
141714	<40 W(h)	<12.3	<0.08
150798	262	>13.4	>2.7
150997	<59	<12.1	<0.23
151680	186	>13.3	>3.3
190406	>100	>13.0	>2.0
191026	>106	>13.0	>1.1
196378	>124	>13.1	>1.9
199951	226	>13.4	>2.6
203387	190	>13.3	>2.1
203608	>108	>13.0	>4.2
209100	<40	<12.0	<0.87
222404	<40	<12.0	<0.20

In the second column of Table III.3.1 are given the upper and lower limits of W(k) - in two cases the k line was noisy and we used W(h). In the third and fourth columns we give the corresponding limits for N(MgII), and for the mean densities along the line of sight, n(MgII) = N(MgII)/d.

From the analysis of the mean densities n(MgII), it is clear that there are strong gradients in MgII distribution in the local gas. The most stringent lower limit, towards β Hyi (HD2151), is in fact two orders of magnitude greater than the most stringent upper limit, towards HD141714. All the upper limits have values which are about 5×10^{-2} the lower limit towards β Hyi. This implies that we are sampling nearby regions with completely different physical states. One can wonder whether the strong variations of n(MgII) are due to variations of the total gas density, or to variations of the ionization state of magnesium. Indeed, the two possibilities are not independent, since the degree of ionization depends on the physical state which in turn is a function of the gas density.

The ionization state of magnesium

MgII is the dominant ionization state of magnesium in the HI regions. Values of the order of or greater than 500 have been found for the ratio [MgII/MgI] in the LISM (Bruhweiler et al. 1984; Centurion et al. 1986). In fact, the interstellar UV flux is able to photoionize MgI even in HI regions, since the ionization potential of MgI (7.6 eV) is lower than the hydrogen ionization limit (13.6 eV). So, unless we are looking through a very dense cold core of a cloud shielded from UV radiation - an unlikely situation in the majority of our lines of

sight - we can neglect the contribution of neutral magnesium to the total magnesium column density.

If the line of sight is sampling a region of very high temperature, it is possible that part of MgII is collisionally ionized to MgIII. In collisional equilibrium MgIII is the dominant form of magnesium at a temperature $T \sim 50{,}000$ K, and even at $T \sim 20{,}000$ K MgIII is already 80% of the total magnesium (Fig. III.3.3; Arnaud and Rothenflug 1985). So, if we do not detect MgII along a line of sight, there are two possibilities: we are sampling a region of very low density or we are sampling a region with a high temperature ($T \gtrsim 20{,}000$ K). These possibilities are not in contrast: assuming as a first approximation pressure equilibrium between the different phases of the ISM, the phases of high temperatures must be characterized by low densities.

Our lines of sight are probably sampling the local diffuse ($n \sim 0.1$ cm^{-3}) warm ($T \sim 10^4$ K) cloud described in Section II.3, where we pointed out the possibility that the local gas has undergone a sudden intense ionization during a transient event during the last $2\text{-}5 \times 10^5$ years. If this local gas is not in ionization equilibrium, it is possible that its degree of ionization is higher than that corresponding to a temperature of 10^4 K, as a consequence of the differences between the cooling time-scales and the recombination time-scales. If this is true, it is possible that the absence of MgII is due to the presence of higher ionization states of magnesium in a gas of only $T \sim 10^4$ K which has not reached the ionization equilibrium.

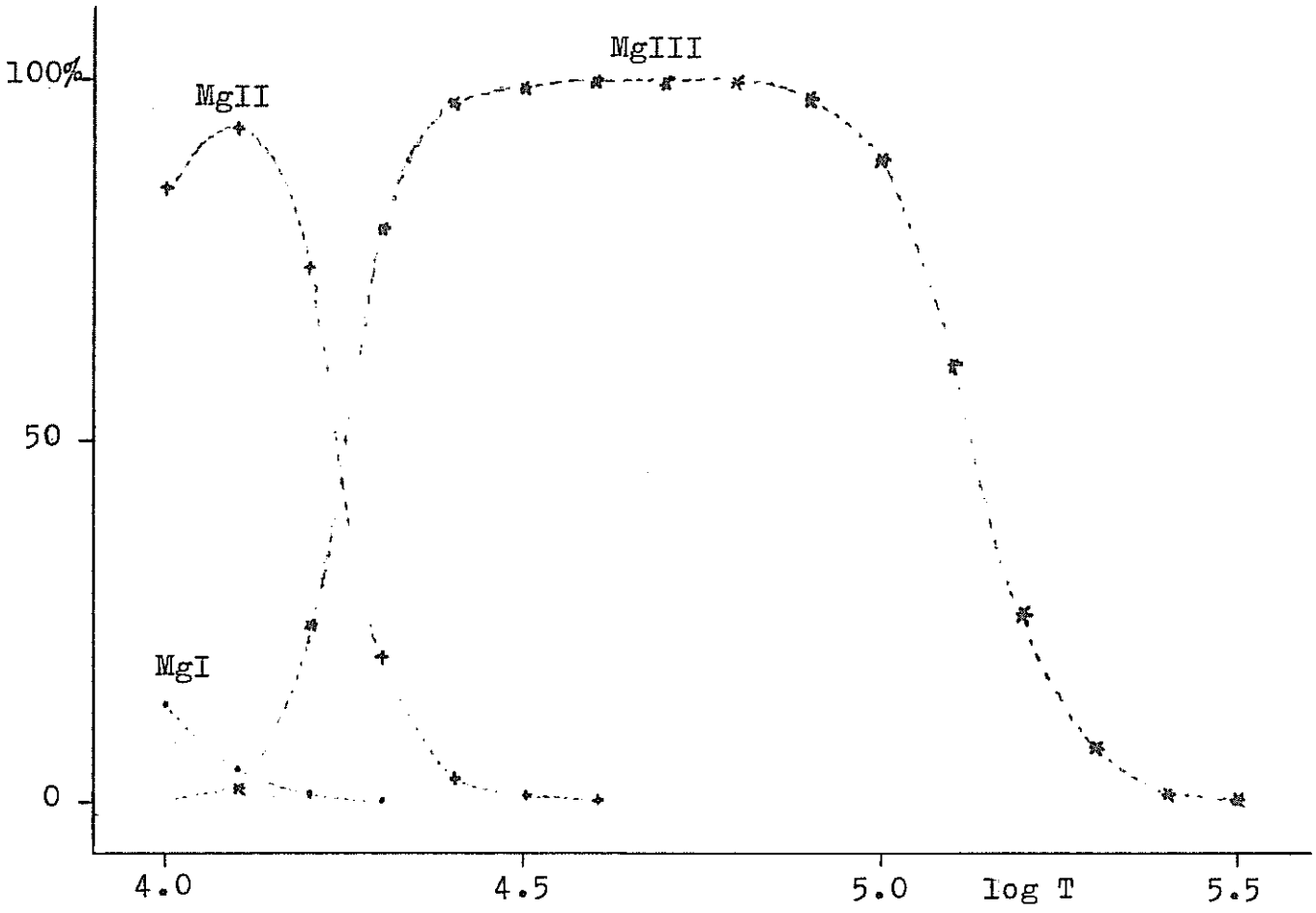

Fig. III.3.3 - Ionization equilibria of the first states of ionization of magnesium (Arnaud and Rothenflug 1985).

We conclude that the very low upper limits of n(MgII) may be the result of the presence along the lines of sight of (1) a high-temperature ($T \gtrsim 20{,}000$ K) low-density gas in collisional equilibrium; (2) a warm ($T \sim 10{,}000$ K) denser ($n \sim 0.1$ cm^{-3}) gas cooling and recombining from an initial state of intense ionization, the cooling time being faster than the recombination time.

Conversion magnesium-hydrogen

In order to derive the total gas density along the lines of sight, and in order to compare our results with the data spread in the literature, we must convert our MgII column densities, to hydrogen column densities, N(H). In doing this, we must
(1) convert N(MgII) to total magnesium column density, N(Mg);
(2) convert N(Mg) to N(H), taking into account the cosmic abundance and the depletion of magnesium from the gas phase to dust grains.

One usually assumes that MgII is the dominant ionization state of magnesium, and so N(Mg) = N(MgII). As we have seen in the preceding paragraph, this assumption breaks down in high-temperature ($T \gtrsim 20{,}000$ K) regions in collisional equilibrium and, possibly, even in warm ($T \sim 10{,}000$ K) gas in a situation of non-equilibrium. If a part of magnesium is in the form of MgIII (or in higher states of ionizations), the above assumption yields an underestimated value of N(Mg). As a consequence, the upper limits of N(MgII) given in Table III.3.1 cannot be considered upper limits for N(Mg), while the lower limits can be treated as conservative lower limits for N(Mg).

Before converting N(Mg) to N(H) we want to treat the problem of

the hydrogen ionization in the general ISM, which may affect the estimates of depletion given in the literature.

Hydrogen ionization and elemental depletion in the ISM

The depletion D of an element X from the gas phase to the dust component of the ISM is defined as:

$$-D = \log [N(H)/N(X)]_{GAS} - \log [H/X]_{COSMIC}, \qquad (3.1)$$

where

$$N(H) = N(HI) + 2N(H_2) + N(HII) \qquad (3.2)$$

is the total hydrogen column density, and N(X) takes into account the contributions of all the ionization states of the element X along the line of sight. Usually it is not possible to apply strictly the definition due to the fact that we cannot observe all the ionization states of the element under study. In particular, it is impossible to measure N(HII) along any line of sight. For this reason, the depletion is practically defined as:

$$-D = \log \left[\frac{N(HI)+2N(H_2)}{N(X)} \right]_{GAS} - \log [H/X]_{COSMIC}, \qquad (3.3)$$

i.e., taking only into account the contributions of neutral atoms and molecules. If we call $\langle x \rangle$ the hydrogen fractional ionization averaged along the line of sight:

$$\langle x \rangle = \frac{N(HII)}{N(HI)+2N(H_2)+N(HII)}, \qquad (3.4)$$

then it is easy to see that the relation (3.1) can be written as:

$$-D = \log \left[\frac{N(HI)+2N(H_2)}{N(X)} \right]_{GAS} + \log[1/(1-\langle x \rangle)] - \log[H/X]_{COSMIC} \qquad (3.5)$$

We conclude that the definition of depletion (3.3), currently used in the literature, yields a value of depletion underestimated by a quantity

$$\Delta = \log[1/(1-\langle x\rangle)]. \qquad (3.6)$$

Let us estimate how much this quantity can affect the value of the depletion along a typical line of sight in the ISM, i.e., along a line of sight which samples all the different phases of the ISM according to their typical filling factors, f. Each phase is characterized by a particular value of fractional ionization, x, and a total hydrogen density per unit volume, n. It is easy to show that the fractional ionization averaged along the line of sight is given by:

$$\langle x\rangle = \left(\sum_i f_i n_i x_i\right)/\left(\sum_i f_i n_i\right) , \qquad (3.7)$$

where the sums are extended over the different phases of the ISM.

Table III.3.2

	CNM	WNM	WIM	HIM
x	0.001	0.15	0.68	1.0
n	42	0.37	0.25	0.0035
f	0.024	~0.18	0.23	~0.57

In Table III.3.2 we report typical values of x, n, and f, taken from the theory of McKee and Ostriker (1977) for the cold neutral (CNM), warm neutral (WNM), warm ionized (WIM) and hot ionized (HIM) regions (Section II.1). Inserting these values in eq. (3.7) we obtain $\langle x\rangle \sim 0.046$, which corresponds to a correction $\Delta = 0.02$ dex. Due to the uncertainties in the measurements of the column densities, this correction is completely negligible, and even if we change slightly the values estimated by McKee and Ostriker, which in any case are in general agreement with the observations, $\langle x\rangle$ will not change

significantly We conclude that along a typical line of sight of the ISM, the correction term (3.6) can be neglected, and the depletions given in the literature are not underestimated. If along a particular line of sight the filling factor of the CNM is greater than its typical value, $\langle x \rangle$ will be smaller, and the correction term Δ even more negligible. Since in this case the average density will be high, we can also conclude that along high-density lines of sight the depletions are not underestimated, since the fraction of ionized hydrogen is negligible.

The problems arise when our line of sight is sampling the warm "intercloud" medium. In fact, in the extreme case in which all the line of sight is contained in a WIM phase, we would have $\langle x \rangle \sim 0.68$ and $\Delta \sim 0.5$ dex. When the mean hydrogen density along the line of sight is $n \gtrsim 0.14$ cm^{-3}, it can be shown (Spitzer 1985) that we are sampling the warm "intercloud" medium, and even if we cannot distinguish between WNM and WIM, the correction term (3.6) is surely not negligible. We conclude that the depletions usually given in the literature can be underestimated up to half order of magnitude along low-density lines of sight (*).

(*) It is knwon from the literature that there exists a direct correlation between the depletion D and the mean density n (e.g., Phillips at al. 1986). This correlation is interpreted in the sense that the higher the density, the less effective are the mechanisms acting for destroying the dust grains. Our conclusion may be the key for a completely different explanation: the lower the mean density, the more underestimated is the true depletion. We do not want to exclude the importance of the mechanisms of dust shielding in high-density gas, but to emphasize that at least a part of the slope in the correlation D-n can be attributed to an underestimation of the depletion along low-density lines of sight.

Magnesium depletion

Murray et al. (1984) made a detailed study of the magnesium depletion towards 74 stars, using improved values for the oscillator strength of the MgII line λ1240 Å, adopting a cosmic ratio log [H/Mg] = 4.46 (Withbroe 1971), and using the definition (3.3) of the preceding paragraph. They found a depletion correlated with the mean density of the gas, n, ranging from about D $\sim$ -0.4 dex (n $\sim$ 0.1 cm^{-3}) to about D $\sim$ -1.0 dex (n $\sim$ 10 cm^{-3}). The uncertainty in the oscillator strength could cause a systematic error of $\pm$ 0.1 dex in these values.

We have adopted the highest value D=-1.0 dex in order to transform the upper limits of N(MgII) to conservative upper limits for N(H). This high value of depletion corresponds to high-density lines of sight and, according to the conclusions of the preceding paragraph, it should not be underestimated: we can use it safely for converting N(Mg) upper limits to N(H) upper limits.

On the other side, we have used the low value D=-0.4 dex in transforming the lower limits of N(MgII). This low value corresponds to low-density lines of sight and, according to the preceding paragraph, it might be underestimated. This would imply that the use of D=-0.4 dex for the conversion magnesium-hydrogen provides a very conservative lower limit for N(H).

Hydrogen densities

Finally, we invert eq. (3.1) for converting N(Mg) to N(H):

$$\log N(H) = \log N(Mg) - \log [H/Mg]_{cosmic} - D \quad . \qquad (3.8)$$

This relation can be rewritten as:

$$\log [\langle y \rangle N(H)] = \log N(MgII) - \log [H/Mg]_{cosmic} - D \quad , \qquad (3.9)$$

where

$$\langle y \rangle = N(MgII)/N(Mg) \qquad (3.10)$$

represents the fraction of MgII over total magnesium, y, averaged along the line of sight. MgII is the dominant form of magnesium ($y \cong 1$) in the cold ($T \sim 10^2$ K) and warm ($T \sim 10^4$ K) interstellar regions; only in hot ($T \sim 10^6$ K) regions should be $y \cong 0$. We can derive a rough estimate of $\langle y \rangle$ for a typical interstellar line of sight using the same arguments used for deriving $\langle x \rangle$ by means of eq. (3.7), and Table III.3.2. Inserting in the equation (*)

$$\langle y \rangle = (\sum_i f_i n_i y_i)/(\sum_i f_i n_i) \qquad (3.11)$$

the values of f and n taken from Table III.3.2, and the above given estimates of y, we obtain $\langle y \rangle \cong 0.998$. Only if the filling factor of the hot phase is close to 1, $\langle y \rangle$ can be significatively smaller than 1. We don't exclude this possibility for our lines of sight, since the sun seems to be situated at the edge of a tenuous cloud embedded in a hot low-density bubble.

(*) In deriving eq. (3.11) we have made the assumption that the ratio [H/Mg] in the gas phase is constant. This assumption is not correct, because the depletion seems to be correlated with the mean density of the gas, nevertheless the use of eq. (3.11) is justified since we need only a rough estimate of $\langle y \rangle$.

TABLE III.3.3

HD	log [<y>N(H)] [cm^{-2}]	[<y>n(H)] [cm^{-3}]
10700	<17.4	<0.024
17925	<17.4	<0.010
25680	<17.4	<0.005
25998	<17.5	<0.005
30495	<17.4	<0.007
39587	<17.5	<0.011
52711	<17.4	<0.005
72905	<17.4	<0.006
82210	<17.4	<0.004
82885	<17.5	<0.011
101501	<17.4	<0.010
111456	<17.4	<0.004
114710	<17.4	<0.011
115383	<17.7	<0.013
120136	<17.5	<0.006
126660	<17.5	<0.008
131156	<17.4	<0.013
141714	<17.7	<0.002
150997	<17.6	<0.004
209100	<17.4	<0.025
222404	<17.4	<0.006

TABLE III.3.4

HD	log N(H) [cm^{-2}]	n(H) [cm^{-3}]
2151	>18.0	>0.056
12929	>17.9	>0.012
29139	>18.2	>0.026
33262	>17.9	>0.022
68456	>18.2	>0.031
71369	>18.3	>0.014
84117	>18.1	>0.031
104979	>18.1	>0.016
131873	>18.5	>0.041
150798	>18.3	>0.055
151680	>18.1	>0.024
190406	>17.9	>0.014
191026	>17.9	>0.008
196378	>18.0	>0.014
199951	>18.2	>0.019
203387	>18.2	>0.015
203608	>17.9	>0.030

In Table III.3.3 we give the upper limits of $\langle y \rangle N(H)$, corresponding to the N(MgII) values reported in Table III.3.1, and to the limits for the depletion assumed in the preceding paragraph. The upper limits of the mean hydrogen density along the line of sight, $n(H)=N(H)/d$, are reported in the last column of the Table, indicated as $\langle y \rangle n(H)$. In Table III.3.4 we give the lower limits of N(H) and n(H). The fact that $\langle y \rangle$ could be < 1 does not affect the validity of these limits. In Fig. III.3.4 we show a projection on the sky (galactic coordinates) of all the targets listed in Table III.3.3. Filled symbols and half-filled symbols correspond respectively to the lower limits and to the upper limits reported in the Table. Above each symbol we give the HD number of the target star, and the estimated upper limit $\langle y \rangle n(H)$ or lower limit n(H). Empty symbols correspond to no measurable column densities.

Discussion

We have compared our upper limits of the total hydrogen densities, n(H), with the values of neutral hydrogen density, n(HI), reported in the literature, and derived from Lyα measurements towards nearby stars. The only star for which we can make a direct comparison is ξ Ind (HD209100). For this line of sight our results are in disagreement with those of McClintock et al. (1978): they found $n(HI) \sim 0.1$ cm^{-3}, while we derive $\langle y \rangle n(H) < 0.025$ cm^{-3} as a conservative upper limit. The discrepancy is more evident if one considers that part of the hydrogen might be ionized, and should be $n(H) > n(HI)$.

Figure III.3.4

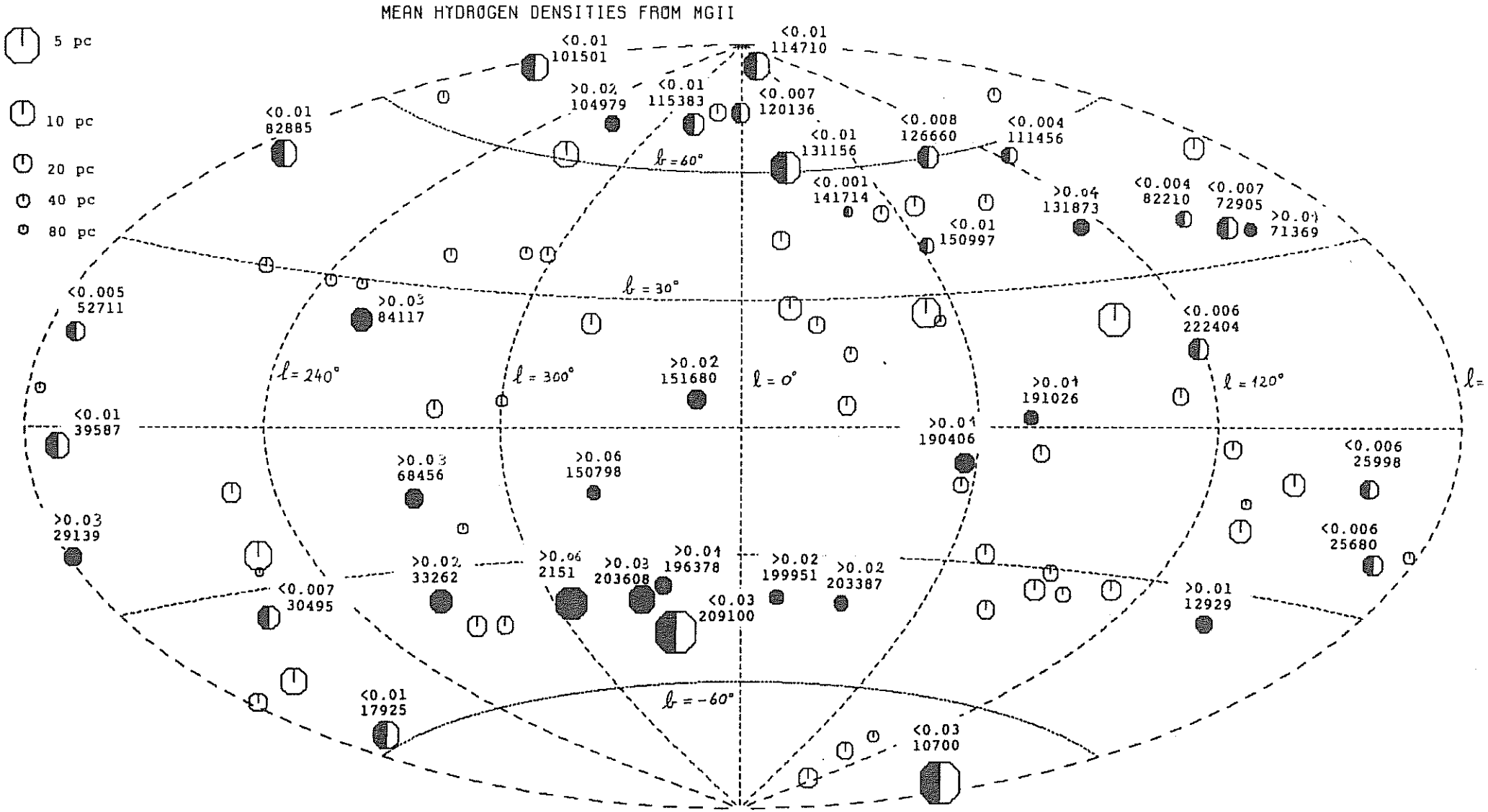

If we interpret this discrepancy as a proof that $\langle y \rangle < 1$, we can estimate an upper limit to $\langle y \rangle$ and, assuming ionization equilibrium, a lower limit to the gas temperature. The comparison of our upper limit with the value of McClintock and co-workers for ξ Ind yields $\langle y \rangle < 0.25$ and $T > 20,000$ K. We exclude this possibility because at $T \sim 20,000$ K only 7% of total hydrogen would be neutral (Arnaud and Rothenflug 1985) and the n(HI) measurement of McClintock et al. (1978) would imply $n(H) \sim 1.5\ cm^{-3}$, in complete disagreement with our upper limit ! We are left with the possibility that the gas along the line of sight is in a particular situation of non-equilibrium. In fact, it is possible that the gas of the local cloud is cooling and recombining from an initial state of intense ionization, as we have pointed out in Section II.3 and in one paragraph of this Section.

A completely different explanation of the above mentioned discrepancy is that the N(HI) measurement by means of the interstellar Lyα is overestimated. In fact, the measurements of the interstellar Lyα in cool stars strongly depend on the adopted line profile for the chromospheric emission. Moreover, the interstellar absorption is strongly saturated, and must be fitted with a Voigt profile which depends on the mean density, n, and on the microturbulence parameter, b. So, the direct HI determinations by means of Lyα absorption in cool stars should be treated with some caution. Moreover, if along the line of sight there are at least two interstellar clouds streaming at different velocities, b and n can be overestimated when fitting the observed absorption profile with a single-cloud model (Vidal-Madjar 1986b).

We have also compared our upper limits with independent n(HI)

determinations along lines of sight close in angle to those investigated by us. For ε Eri (ℓ=196°, b=-48°, d=3.3 pc), McClintock et al. (1978) find a best fit to the observed Lyα profile for 0.10 cm^{-3} < n(HI) < 0.16 cm^{-3}. We find $\langle y \rangle n(H) < 0.04$ cm^{-3} for the angularly close star HD 19994 (ℓ=182°, b=-47°, d=18 pc). In this case our low value could be explained as due to a real decrease of the gas density beyond ε Eri. In fact, Anderson and Weiler (1978) find n(HI) = 0.005 ± 0.002 cm^{-3} towards HR1099 (ℓ=185°, b=-41°, d=33 pc). All these results are consistent with the presence of a tenuous (n ~ 0.1 cm^{-3}) cloud which surrounds the sun and terminates at a distance 3.3 pc < d < 18 pc in the region of the sky around ε Eri.

We find a similar situation comparing α CMi (ℓ=214°, b=+13°, d=3.5 pc), for which Anderson et al. (1978) give n(HI) ~ 0.09-0.13 cm^{-3}, with HD52711 (ℓ=187°, b=+15°, d=17 pc), for which we derive $\langle y \rangle n(H) < 0.005$ cm^{-3}. In this case the edge of the cloud should be situated immediately after α CMi and, even so, the two results are not consistent: we have another indication that either $\langle y \rangle < 1$, or that n(HI) has been overestimated.

For what concern our lower limits, the only line of sight for which we have a comparison with direct hydrogen determinations is towards α Tau (HD29139): McClintock et al. (1978) find n(HI) < 0.15 cm^{-3}, and we find n(H) > 0.03 cm^{-3}: the two results are consistent, even if not stringent. Generally, our lower limits are not stringent: the majority of them is in the range 0.01 cm^{-3} to 0.03 cm^{-3}, while the global review of Paresce (1984) indicates that the local cloud has a mean density of about 0.07 cm^{-3}. This is not too

surprising, due to the combined effect of (1) assuming a conservative value for the degree of saturation of the MgII doublet, (2) the possibility that the depletion is underestimated, and (3) the possibility that $\langle y \rangle < 1$. Nevertheless, these results are useful in order to study the global hydrogen distribution in a radius of few tens of parsecs of the sun.

In the galactic longitude range from $\ell = 0^\circ$ to $\ell = 90^\circ$ and at low galactic latitudes the high density towards HD 190406 is in agreement with the large column densities reported in the literature (Paresce 1984) towards α Oph ($\ell = 36^\circ$, $b = +23^\circ$, d=17 pc). A completely different pattern is observed at higher latitudes where there are many stars for which $n(H) < 0.01$ cm^{-3}. The most interesting case is that of HD 141714, which gives a $n(H) < 0.002$ cm^{-3} value, in agreement with that found towards the white dwarf HZ43 (Paresce 1984). At negative latitudes there are two stars at about 30 pc with $n(H) > 0.01$ cm^{-3} limiting the extension of the low density region.

In the quadrant defined by ℓ ranging from 90° to 180° we do not find any trace of the strong density gradient visible in the first quadrant at low latitudes: the star HD25998 (d=20 pc) does not show any significant interstellar absorption, while at slightly shorter distances HD168723 and HD190406 do.

At galactic longitudes between $\ell = 170^\circ$ and $\ell = 240^\circ$, independently of latitude and distances, all the targets show intrinsically low densities, confirming the presence of a large hole. A remarkable exception is the strong absorption observed towards HD 29139, which is not seen at all in HD 25680, which is angularly close.

Finally, in the quadrant from $\ell = 270^{\circ}$ to $\ell = 360^{\circ}$ all the targets show strong absorptions for all latitudes and even at very short distances, as it is the case of β Hyi.

Our results suggest that the sun is embedded in a low density volume with a typical density of $n(H) < 0.01$ cm^{-3}. β Hyi at d=6.3 pc is the closest star in our sample which shows a strong absorption, but the absence of any feature towards ε Ind at d=3.5pc gives $n(H) < 0.025$ cm^{-3}, which implies a considerable increase in the gas density beyond ε Ind.

References

Anderson,R.C., Weiler,E.J.: 1978, Astrophys. J., 224, 143.

Anderson,R.C., Henry,R.C., Moos,H.W., Linsky,J.L.: 1978, Astrophys. J., 226, 883.

Arnaud,M., Rothenflug,R.: 1985, Astron. Astrophys. Suppl., 60, 425.

Bertaux,J.L.: 1984, in Local Interstellar Medium, IAU Coll. 81, NASA CP-2345, p. 3.

Bohm-Vitense,E.: 1981, Astrophys. J., 244, 504.

Crutcher,R.M.: 1982, Astrophys. J., 254, 82.

Bruhweiler,F.C., Kondo,Y.: 1982, Astrophys. J., 259, 232.

Bruhweiler,F.C., Oegerle,W., Weiler,E., Stencel,R., Kondo,Y. : 1984, in Local Interstellar Medium, IAU Coll. 81, NASA CP-2345, p. 64.

Centurion,M., Vladilo,G., Molaro,P., Beckman,J.E. : 1986, Proc. XXVI COSPAR meeting, Toulouse, July 1986, Symposium no. 7, in press.

Cowie,L.L., Songaila,A.: 1986, Ann. Rev. Astron. Astrophys., 24, 499.

Ferlet,R., Lallement,R., Vidal-Madjar,A. : 1986, Astron. Astrophys., 163, 204.

Franco,M.L., Crivellari,L., Molaro,P., Vladilo,G., Ramella,M., Morossi,C., Allocchio,C., Beckman,J.E.: 1984, Astron. Astrophys. Suppl., 58, 693.

Kondo,Y., Talent,D.L., Barker,E.S., Dufour,R.J., Modisette,J.L.: 1978, Astrophys. J., 220, L97.

McClintock,W., Henry,R.C., Linsky,J.L., Moos,H.W.: 1978, Astrophys. J., 225, 465.

Molaro,P., Vladilo,G., Beckman,J.E.: 1986, Astron. Astrophys., 161, 339.

Murray,M.J., Dufton,P.L., Hibbert,A., York,D.G.: 1984, Astrophys. J., 282, 481.

Paresce, F.: 1984, Astron. J., 89, 1022.

Reimers,D.: 1977, Astron. Astrophys., 57, 395.

Spitzer,L.: 1968, Diffuse Matter in Space, Interscience Publishers, John Wiley and Sons, p. 19.

Spitzer,L.: 1985, Astrophys. J., 290, L21.

Vidal-Madjar,A., Ferlet,R., Gry,C., Lallement,R.: 1986a, Astron. Astrophys., 155, 407.

Vidal-Madjar,A.: 1986b, private communication.

Vladilo,G., Beckman,J.E., Crivellari,L., Franco,M.L., Molaro,P.: 1985, Astron. Astrophys., 144, 81.

Weaver,H.: 1979, in The Large Scale Characteristics of the Galaxy, IAU Symp. 84, ed. W.B.Burton (Dordrecht:Reidel), p. 295.

Wiese,W.L., Smith,M.W., Miles,B.M.: 1969, Atomic Transition Probablities, NSRDS-NBS 22.

Withbroe,G.L.: 1971, The Menzel Symposium, ed. K.B. Gebbie, NBS SP-353, p. 27.

APPENDICES

1. COOLING MECHANISMS IN THE ISM

The most important processes leading to energy losses in the ISM involve collisions between particles followed by photon emission. We assume that once the photon is emitted, its energy is lost for the gas. A sufficient, but not necessary condition is that the gas is optically thin to all emitted photons. We also assume that electrons and ions share a common Maxwell-Boltzmann distribution of kinetic energy at some temperature T. By convention we term "internal energy" the microscopic kinetic energy of the gas particles; excitation and ionization energies are considered "external" to the system with this kind of convention.

The energy lost by the gas per unit volume and unit time is a function of the temperature, the ionization structure, the density and the chemical composition of the gas, called the "cooling function".

For equal kinetic energies, an electron is more efficient than an ion in exciting an atomic transition with an energy jump of order kT, because its collisional timescale is better matched to the atomic timescale. Therefore collisions involving electrons will dominate the cooling rate, unless their abundance is low. The next lightest and most abundant species effective for collision is hydrogen.

In a partly ionized gas of cosmic abundance, cooling at high temperatures is mainly due to electron impact excitation of electronic

levels of the neutral and ionized constituents, and cooling at low temperatures is due mainly to electron impact excitation of fine structure levels of the neutral and ionized constituents. With decreasing fractional ionization, fine structure excitation by neutral hydrogen impacts becomes important. The cooling efficiency can be significantly modified by the presence of molecular species in the gas.

In Fig. A1.1, taken from Dalgarno and McCray (1972), are shown the contributions of the most abundant interstellar species to the cooling of the gas by electron impact excitations, as a function of the kinetic temperature, T. It is clear how the abundances in the gas phase (and hence the depletions) can affect the total cooling function. At low temperatures, the fine-structure excitation of CII controls the cooling. As the temperature increases, fine-structure excitation of SiII and FeII occur more efficiently than of CII. Above 600 K, metastable excitation of FeII, and above 6000 K, metastable excitation of OI, NI, CII, SiII and SII, are all effective in cooling. The cooling due to excitation of atomic hydrogen increases very rapidly with temperature and completely controls the cooling above 10500 K.

In Fig. A1.2, from the same authors, are shown some cooling functions which include the contributions of the most abundant species and the effects of neutral hydrogen impact excitation. The different cooling functions are the result of the adopted value for the fractional ionization $x = n_e/n$. For $x > 10^{-2}$, the cooling function depends linearly upon x, because electron impact excitations are the dominant cooling processes. For $x < 10^{-3}$, the cooling function below

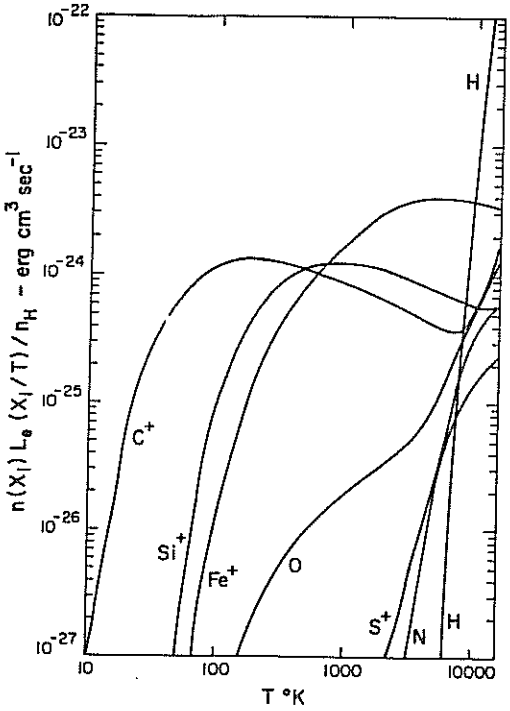

FIGURE A1.1 - The individual contributions to the interstellar cooling by electron impact excitations.

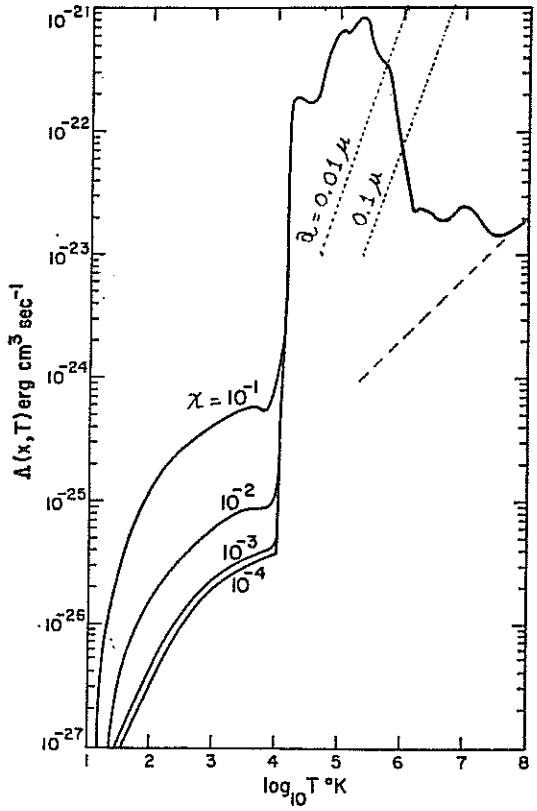

FIGURE A1.2 - The interstellar cooling function for various values of the fractional ionization x.
Dashed line: bremsstrahlung cooling.
Dotted lines: cooling by interstellar grains for 2 values of the grain radius a.
See text for references.

1000 K is independent of x, because hydrogen atom impact excitation control the cooling.

As the temperature increases further, thermal ionization alters the ionization structure of the gas. Excitation of the excited levels of atomic hydrogen becomes unimportant as HI disappears, and excitations to metastable and allowed levels of various ionization states of such constituents as He, C, O, N, Ne, Si, Fe and Mg control the thermal balance over a wide temperature range up to about 10^7 K.

Above 10^7 K, bremsstrahlung dominates. In fact, if the temperature is so high that the gas is completely ionized, collisional excitation/ionization is not present and free-free losses start to dominate energy losses. It is important to note that bremmstrahlung is an inefficient cooling mechanism (see dashed line in Fig. A1.2; Lazareff 1982), so, once a gas is heated to very high temperatures ($T > 10^6$ K), its cooling time will be very long ($t_{cool} > 10^6$ years).

Dust grains provide another energy sink. Ions or electrons hitting dust grains transfer to them part of their kinetic energy; the grains achieve thier energy balance by radiating in the infrared. The actual computation of dust cooling is quite complicate: grain charge, grain transparency (for small grains and high energy particles), and grain destruction by sputtering, must all be taken into account. Dust cooling is efficient at high temperatures (see dotted curves in Fig. A1.2; Lazareff 1982), but is limited by grain destruction, so its importance can be assessed only in specific situations.

Time-dependent cooling

Time-dependent models are characterized by discrete bursts of radiation or supersonic shocks that ionize and heat the interstellar gas. In the absence of additional heat sources, the plasma cools more rapidly than it recombines. An important consequence of this effect is that, at a given temperature the degree of ionization predicted by time-dependent models usually exceed those predicted by steady-state models. Kafatos (1973) calculated the time-dependent cooling functions between 10^4K and 10^6 K for the situation in which the ionization relaxes from an initial stage determined by thermal equilibrium at 10^6 K, and he showed that at 10^4 K most of the hydrogen is still ionized.

2. STATIONARY HEATING MECHANISMS IN THE ISM

The main heating mechanisms in the ISM are due to ionization of the gas by means of an external source. The sources which provide a stationary ionization of the gas are the interstellar radiation field and the cosmic-ray flux. If we call E the energy of the incoming particle (photon or cosmic-ray), and IP the ionization potential of the ionized atom or ion, each ionization yields an electron with a kinetic energy (E-IP) which is in part redistributed as thermal energy of the gas (elastic collisions) and in part lost due to collisional excitations and ionizations.

Also the presence of dust can provide stationary heating mechanisms, such as photoelectric emission from dust grains and

formation of molecular hydrogen on grains.

UV Photoionization

The photoionization of an abundant atom or ion X

$$h\nu + X \longrightarrow X^{+} + e$$

yields an electron of energy ($h\nu$-IP), where IP is the ionization potential of X. Because the radiation field terminates at the Lyman limit, ($h\nu$-IP) does not exceed 5.7 eV and its mean value for a gas of cosmic abundance is 2.1 eV (Dalgarno and McCray 1972). The electrons lose energy mainly in elastic collisions with the ambient electron gas. The energy loss occurs rapidly and thermalization is achieved well before the electrons are removed by recombination.

Soft X-rays photoionization

The absorption of sof X-rays yields fast photoelectrons that lose energy in ionizing, exciting and heating the interstellar gas. Direct heating of the free electrons is negligible. Absorption by He assumes a major role because its cross sections towards X-rays are substantially larger than the H cross sections. In a highly ionized gas, the heat per photon is equal to the kinetic energy of the photo-electron. In a weakly ionized gas, the photoelectron causes further ionizations and the heating efficiency is decreased. In the limit of vanishing fractional ionization, the heat deposited by the absorption of a 50-eV photon is 6 eV, and by the absorption of a 200-eV photon is 23 eV.

Cosmic ray ionization

A critical point about the computation of cosmic rays ionization rates is that, due to the interplanetary magnetic field and due to the solar wind, we cannot measure the energy distribution of the low energy cosmic rays, which give the main contribution to ionization. The main ionization reaction

$$p + HI \longrightarrow p + p + e$$

produces an energetic secondary electron. For a 2 MeV incoming proton the mean energy of the secondary electron is 32 eV. In a weakly ionized gas, the secondary electron loses energy in ionizations and excitations until its energy falls below 10.2 eV, and only the remaining energy is redistributed in elastic collisions. On average, therefore, a heat source of less than 10 eV is associated with each primary ionizing element. In a highly ionized gas the secondary electron mainly redistributes its energy in elastic collisions with the ambient electron gas.

The cosmic rays heat the free electrons also by direct elastic collisions. For fractional ionization $x > 0.1$ direct collisions provide a more efficient heating mechanism than ionization followed by emission of secondary electron.

Photoemission from dust grains

Watson (1972) investigated the consequences of photoemission from interstellar grains in HI regions. For likely grain materials (except ice), the photoemission is expected from laboratory data to be

relatively efficient for photon energies $h\nu \sim$ 10-13.6 eV. The ejected photoelectrons represent an energy input into HI clouds comparable to that from low-energy cosmic rays or soft x-rays. Process is self-limited due to positive charging of grains. Jura (1976) has suggested that the photoelectric effect from very small grains may supply the heating required to mantain diffuse interstellar clouds at temperatures near $T \sim 80$ K. The heating model could also explain the existence of a warm neutral "intercloud" medium.

Formation of H2 molecules on grains

Hydrogen molecules can form as a result of H atoms impacts on grains. Each such molecule formation releases a binding energy of 4.48 eV, which must go partly into heating the grain, partly into overcoming the energy of adsorption to the grain surface, partly into excitation energy of the newly formed molecule, and partly into the translational kinetic energy with which the molecule leaves the grain. Detailed computations (Glassgold and Langer 1974) indicate that even if almost all the binding energy appears in the form of molecule kinetic energy, this process could account for an equilibrium temperature of about 80 K only with considerable straining of the parameters involved (Spitzer 1978).

References

Dalgarno,A., McCray,R.A., 1972, Ann. Rev. Astron. Astrophys., 10, 375.

Field,G.B., Goldsmith,D.W., Habing,H.J., 1969, Astrophys. J., 155, L149.

Field,G.B., 1974, Atomic and Molecular Physics and the Interstellar Matter, eds. Balian at al., p. 467.

Glassgold,A.E., Langer,W.D., 1974, Astrophys. J., 193, 73.

Jura,M.: 1976, Astrophys. J., 204, 12.

Kafatos,M.: 1973, Astrophys. J., 182, 433.

Lazareff,B., 1982, Diffuse Matter in Galaxies, eds. Audouze et al., p. 141.

Silk,J., 1973, Pub. Astron. Soc. Pacific, 85, 704.

Spitzer, L., Jr., 1978, Physical Processes in the Interstellar Medium, John Wiley and Sons, Inc., p. 131-148.

Watson,W.D.: 1972, Astrophys. J., 176, 103.

3. TIME DEPENDENT HEATING MECHANISMS IN THE ISM

Here we briefly describe the interactions between stars and ISM which are responsible for the existence of the hot interstellar gas. It is important to understand that, even if these mechanisms do not give a stationary energy input to the ISM, once a hot ($T \sim 10^6$ K) region is created, it will persist for a long time ($t_{cool} > 10^6$ years) due to the inefficiency of the radiative cooling at high temperatures.

Supernovae and Supernova Remnants

Of the possible sources of high-temperature and high-velocity gas in the ISM, supernovae are almost certainly dominant. The interaction of supernova remnants (SNR) with the ISM has been treated in detail by Woltjer (1972) and Chevalier (1977). Here we report the main steps in the evolution of a typical SNR with an initial kinetic energy of $E_o = 10^{51}$ erg, an ejected mass of $M_o = 0.25\ M_\odot$, an initial velocity of 20,000 km/s, in an homogeneous ISM with a density of $n_o = 1\ cm^{-3}$, as reviewed by Lamers (1982).

At first the ejecta expand freely without any effect of the ISM. This free-expansion phase ends when the amount of swept-up interstellar gas becomes comparable to M_o, i.e. when

$$\frac{4}{3}\pi R^3 \rho_o = M_o \qquad \text{(A3.1)}$$

or R = 1.2 pc. This is already after 60 years. This time-scale,

combined with the small distance covered by the SNR in the ISM at this stage, imply that this first phase cannot significatively affect the ISM.

The next phase is called adiabatic, and was described in detail by Sedov (1959). During this phase the mass of the expanding shell almost totally consists of swept-up interstellar material. As the shell expands supersonically into the ISM, the shock between the ISM and the shell will heat the shell to a temperature of 10^7 K. This temperature is so high that radiative cooling can be neglected (see Appendix 1), and the shock can be considered adiabatic. The structure of the SNR during this phase consists of a inner region which was heated when the shock passed through it and contains hot interstellar gas at low density. This hot bubble is surrounded by the expanding shell of swept-up interstellar gas. The shell expands because it has still a large fraction ($\sim$ 28%) of the initial kinetic energy. The shell radius is given by (Sedov 1959):

$$R_S \sim 13\ (E_{51}/n_o)^{1/5}\ t_4^{2/5}\ \text{pc} \qquad \text{(A3.2)}$$

where $E_{51} = E_o/(10^{51}\ \text{erg/s})$ and t_4 is the expansion time expressed in units of 10^4 years. The adiabatic phase ends when the shell temperature has decreased to $< 10^6$ K, because then radiative cooling becomes important. This happens about after 3×10^4 years; at this stage the shell has a radius $R_S \sim 20$ pc. Of course these parameters considerably change if the SNR expands in a low-density bubble of the ISM previously generated by the action of strong stellar winds.

When radiative losses become important the shell will rapidly cool to a low temperature (10^2-10^4 K). The shock between the shell and

the ISM will be nearly isothermal, which results in a high compression rate and produces a thin high density shell. In this isothermal phase the thin shell expands with a constant momentum, as a pressure driven snowplough, according to the law

$$R_s \sim 8.4\ (R_c^2 E_{51}/n_o)^{1/7}\ t_4^{2/7}\ \text{pc} \qquad \text{(A3.3)}$$

(McKee and Ostriker 1977), where R_c is the shell radius at the end of the adiabatic phase. The snowplough phase will end when the velocity of the shell becomes comparable to the mean velocity of the interstellar clouds ($\sim$ 10 km/s). After that time the SNR breaks up by interaction with the ISM and looses its identity.

Each supernova adds about 3% of its initial kinetic energy to the ISM. The other 97% is used for heating the hot bubble, and part of it is later radiated away during the radiative cooling of the shell. Even if the ejected material is spherically symmetrical and propagates through a homogeneous ambient medium, one can expect that the remnant will be clumpy because it is subject to Rayleigh-Taylor instabilities.

Stellar winds

Another mechanism producing high-velocity and high-temperature interstellar gas is the action of winds from OB stars on the ISM. Castor et al. (1975) and Weaver et al. (1977) have studied the stucture and evolution of the interstellar bubble that is created by such stellar winds. This is similar to the formation of a bubble by a supernova. The main difference between the two type of processes is

that a stellar wind provides a constant energy and mass supply over a period of 10^6-10^7 years, whereas a SN explosion is an instantaneous ejection where all the energy and mass is released at once. Also in this case we can distinguish three phases (free expansion, adiabatic expansion and snowplough), but only the third one is relevant for the ISM. In fact, a wind with a velocity of 2000 km/s and a kinetic energy of 10^{36} erg produce a bubble which, at the end of the adiabatic phase (a few thousand years after the star has "switched on" the wind), has an outer radius of only $R \sim 0.6$ pc.

In the snowplough phase the bubble complex has the following structure: (1) the stellar wind close to the star; (2) a hot bubble which is still too hot to suffer radiative cooling and so it will continue to expand adiabatically; (3) a thermal conduction layer at the boundary with a cold shell. The radius of the bubble is given by the relation (Weaver et al. 1977):

$$R \sim 28 \, (L_{36}/n_o)^{1/5} \, t_6^{3/5} \ \text{pc} \ , \qquad \text{(A3.4)}$$

where L_{36} is the wind luminosity in units of 10^{36} erg/s, n_o is the density of the ISM surrounding the bubble and t_6 is the expansion time in units of 10^6 years.

This model has some interesting observational consequences: the hot bubble ($T \sim 1.6 \times 10^6$ K) is a source of soft X-rays and the conduction layer between the cold shell and the hot interior may produce absorption lines which are typical of gas at $T \sim 10^5$-10^6 K, e.g. OVI and NV lines.

References

Castor,J., McCray,R., Weaver,R.: 1975, Astrophys. J., 200, L107.

Chevalier,R.A.: 1977, Ann. Rev. Astron. Astrophys., 15, 175.

Lamers,J.G.L.M.: 1982, Diffuse Matter in Galaxies,
Eds. Audouze et al., p. 35.

Lamers,J.G.L.M.: 1982, Diffuse Matter in Galaxies,
Eds. Audouze et al., p. 45.

McKee,C.F., Ostriker,J.P.: 1977, Astrophys. J., 218, 148.

Sedov,L.: 1959, Similarity and dimensional methods in mathematics,
New York: Academic.

Woltjer,L.: 1972, Ann. Rev. Astron. Astrophys., 10, 129.

Weaver,R., McCray,R., Castor,J., Shapiro,P., Moore,R.: 1977,
Astrophys. J. 218, 377.